ASSESSMENT OF A NEXT GENERATION GRAVITY MISSION FOR MONITORING THE VARIATIONS OF EARTH'S GRAVITY FIELD

TN2: SYSTEM DRIVERS

Written by	***Responsibility*** + handwritten signature if no electronic workflow tool
A. Anselmi	Author (on behalf of the TAS-I study team)
Verified by	
S. Cesare	Head of TAS-I BLOOS Business Acquisition and Advanced Projects
Approved by	
A. Anselmi	Study Manager
Documentation Manager	
R. Cavaglià	

Approval evidence is kept within the documentation management system.

CHANGE RECORDS

ISSUE	DATE	§ CHANGE RECORDS	AUTHOR
01	4-12-09		aa

TABLE OF CONTENTS

1. INTRODUCTION

1.1 Scope and Purpose

This document is submitted in fulfilment of WP 1200 of the Next Generation Gravity Mission (NGGM) study. Its purpose is to complement the review of the scientific requirements, provided as output of WP1100 [RD-12], with a critical review of the key implementation requirements and constraints of a satellite mission based on low-low Satellite to Satellite Tracking (ll-SST) by laser interferometer. As an outcome of the review, criteria for payload and mission selection are proposed.

2. DOCUMENTS

2.1 Applicable Documents

[AD-1] Assessment of a Next Generation Gravity Mission to monitor the variations of Earth's gravity field, Statement of Work, EOP-SF/2008-09-1334, Issue 2, 20 November 2008, Appendix 1 to AO/1-5914/09/NL/CT

[AD-2] Special Conditions of Tender, Appendix 3 to AO/1-5914/09/NL/CT

[AD-3] Draft Contract. Appendix 2 to AO/1-5914/09/NL/CT.

2.2 ESA Reference Documents

[RD-1] Rummel et al. (2003), Scientific objectives for Future Geopotential Missions, Technical Note, Version 6 from the ESA contract No: 16668/02/NL/MM "Enabling Observation Techniques for Future Solid Earth Missions"

[RD-2] Koop, R., Rummel, R. (2007), The Future of Satellite Gravimetry, Final Report of the Future Gravity Mission Workshop, 12-13 April 2007 ESA/ESTEC, Noordwiik, Netherlands

[RD-3] Laser Doppler Interferometry Mission for determination of the Earth's Gravity Field, ESTEC Contract 18456/04/NL/CP, Final Report, Issue 1, 19 December 2005

[RD-4] Laser Interferometry High Precision Tracking for LEO, ESA Contract No. 0512/06/NL/IA, Final Report, July 2008

[RD-5] System Support to Laser Interferometry Tracking Technology Development for Gravity Field Monitoring, ESA Contract No. 20846/07/NL/FF, Final report, September 2008

[RD-6] Bender P.L., Wiese D.N., and Nerem R.S., "A Possible Dual-GRACE Mission With 90 Degree And 63 Degree Inclination Orbits", Proceedings of the 3rd International Symposium on Formation Flying, Missions and Technologies, Noordwijk (NL), April 2008

[RD-7] T. van Dam et al., Monitoring and Modelling Individual Sources of Mass Distribution and Transport in the Earth System by Means of Satellites, Final Report, ESA Contract No. 20403, November 2008

[RD-8] Variable Earth Model Description and Product Specification Document, ESA Contract No. 20403, November 2008

[RD-9] Enabling Observation Techniques for Future Solid Earth Missions, ESA Contract No: 16668/02/ NL/MM, Final report, Issue 2, 15 July 2004.A

2.3 Further Reference Documents

[RD-10] GOCE Flight Acceptance Review, Industry Presentation, ESTEC, 4 March 2008

[RD-11] GRACE Proposal to NASA's Earth System Science Pathfinder Program, 10 December 1996

[RD-12] WP1100 Report, University of Luxembourg, November 2009

[RD-13] Sneeuw, N. and Schaub, H.P., Satellite Clusters for Future Gravity Field Missions, IAG International Symposium Gravity, Geoid and Space Missions, Porto, Portugal Aug. 30 – Sept. 3, 2004

[RD-14] Future Solar Activity Estimates for Use in Prediction of Space Environmental Effects On Spacecraft, NASA, Marshall Space Flight Center, Huntsville, Alabama, Nov. 2009

3. REQUIREMENTS REVIEW AND IDENTIFICATION OF SYSTEM DRIVERS

3.1 Introduction

The future mission subject of this study is loosely defined, relative to the current generation of gravity missions, GRACE and GOCE, as possessing the following characteristics:

- main instrument based on low-low SST measurements (GRACE-like);
- improved instrument sensitivity/accuracy, 100 to 1000 times better than GRACE;
- high spatial resolution, comparable to GOCE;
- high time resolution, better than GRACE;
- mission duration comparable to GRACE (GRACE was initially proposed for 5 years; it was launched on March 17, 2002 and it is expected to operate at least until 2012).

Defining exactly the mission objectives outlined above is one of the purposes of this study. The mission requirements listed above are intertwined. Designing for time resolution (e.g., a repeat orbit with a short repeat rate) automatically leads to poor spatial resolution. Optimizing for spatial resolution, as GOCE does, leads to poor time sampling. High resolution in both space and time may be achieved by a multiple satellite configuration such as a number of GRACE-like pairs in different orbits. Such a concept, however, will at some point exceed the available level of resources. Payload costs, in turn, are driven by the sensitivity / accuracy requirement and mission operations costs are driven by mission duration. As usual, the mission definition shall occur by a trade-off of scientific mission requirements and implementation constraints, including cost constraints.

The parameters defining a mission architecture are defined below. This review of the satellite implementation requirements will initial focus on a GRACE-like mission architecture featuring 2 satellites on the same orbit, separated by a convenient distance and linked by a laser interferometer system. Extension to multiple-pair constellations will then be straightforward.

3.2 Parameters defining a mission architecture

The parameters defining a mission architecture include:

- Number and type of orbits
- Number of orbiting satellites
- Mission duration
- Satellite formation geometry
- Payload instruments for the gravity field measurement
- Drag free control.

They are defined and briefly discussed below.

3.2.1 Number and type of orbits

To reduce the level of temporal aliasing in the gravity field solution, the frequency by which the whole Earth surface is sampled at the resolution of the phenomena to be monitored must be increased (independently of the gravity field measurement accuracy). A straightforward way to reduce the time needed for a global sampling of the Earth surface is to distribute the gravimetric satellites on different orbits. The effectiveness of the sampling depends also on the orbit type.

For instance, an effective use of two orbits has been identified by Bender [RD-6]: with two circular orbits at 312 km altitude and inclination i1 = 90° (4.986 day repeat period) and i2 = 62.7° (22.69 day repeat period) respectively, it is possible to achieve a quite uniform and fast coverage of the Earth surface in N-S and E-W directions, permitting solutions for fairly rapid time variations in the gravitational potential (even for periods as short as one day, in the polar regions). The ground coverage density improvements produced by this orbit combination, with respect to a single orbit (the GOCE orbit is taken as reference), is shown in Figure 3.2-1.

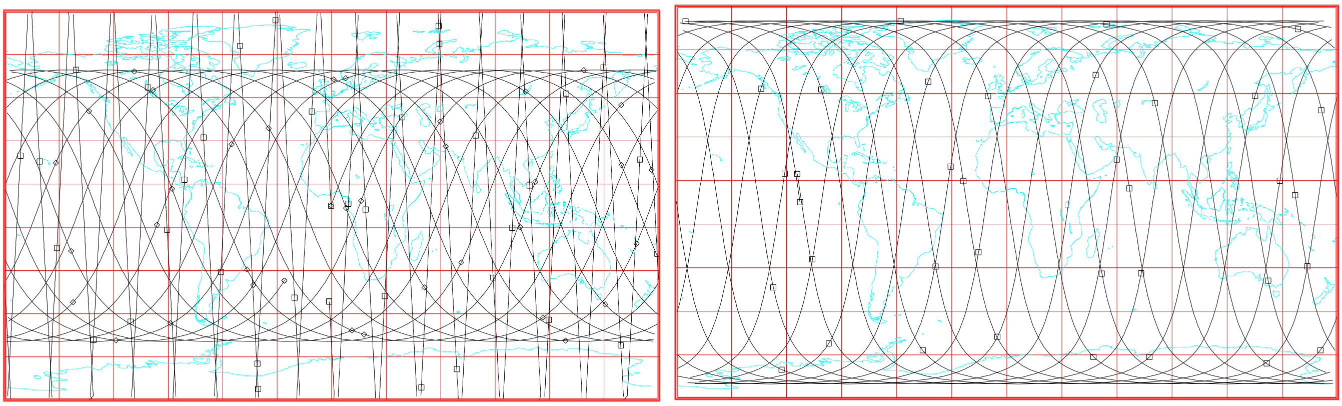

Figure 3.2-1 : 1-day Earth surface coverage of the Bender formation (left) and the GOCE orbit (right)

A multi-orbit scenario is clearly a design driver whose impact depends on the number and type of involved orbits. For instance, the satellite deployment on the two orbits proposed in [RD 6] requires two independent launches with VEGA. The restartable upper stage of the VEGA launcher has not enough linear impulse (~1600 kNs) to release a first set of satellites on a 312 km, 90° orbit, and then to perform an inclination change of 27.3° (ΔV = 3.64 km/s) for releasing the second satellite pair on the 62.7° orbit. Soyuz-Fregat may be an alternative.

From a scientific standpoint, the orbit altitude must be as low as possible. The altitude, hence the air density, is the sizing factor, together with the mission duration and the satellite cross section, of the on-board propulsion system in charge of orbit maintenance, and of the power generation system if electric propulsion is utilized. As an example, Figure 3.2-2 shows the amount of Xenon propellant for drag compensation by ion thrusters, in 5 and 10 years, and the mission lifetime over which the drag force can be compensated with 40 kg of Xenon (the amount carried on GOCE), as function of the mean orbit altitude. A satellite cross section of 1.1 m² is considered (GOCE case), and the worst-case solar flux forecast is assumed.

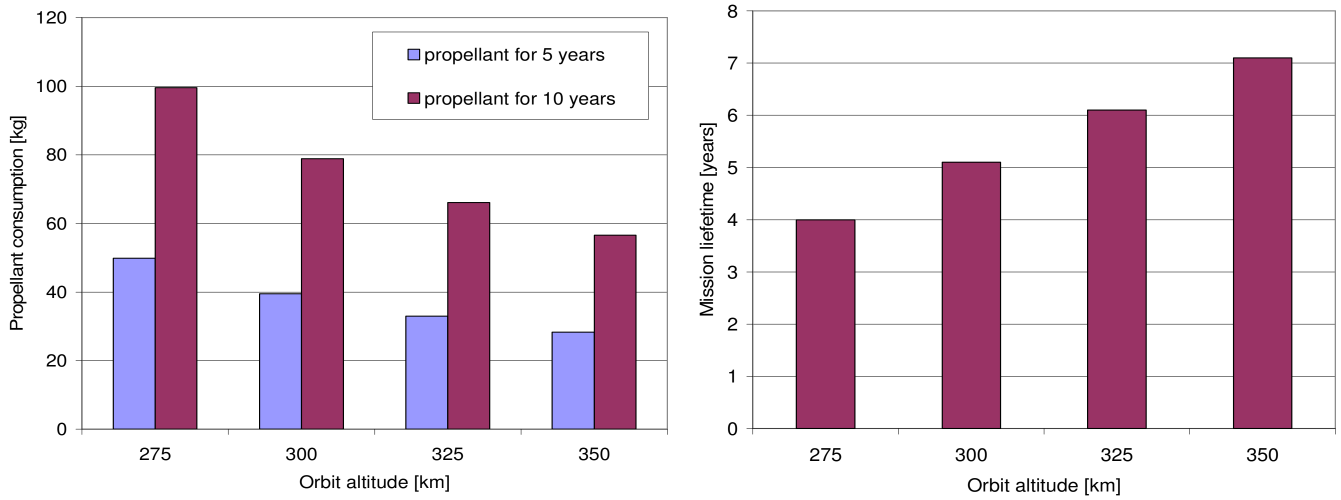

Figure 3.2-2 : Propellant consumption for drag compensation vs. orbit altitude (left) and mission lifetime with drag force compensation achievable with 40 kg of propellant (right)

The orbit inclination determines the latitude belt covered in the gravity field sampling. A polar orbit (i = 90°) is desirable for covering the whole Earth surface, including the polar regions themselves. The combination of a polar orbit with a medium inclination orbit has been proposed for achieving a dense and uniform coverage in short time periods [RD-6]. The orbit inclination impacts the satellite design via the rotation of the orbit plane, that can be synchronous or not with the Earth rotation around the Sun. The sun-synchronous condition (that implies a well defined inclination > 90° as function of the orbit altitude) is preferred from an engineering viewpoint because it produces nearly constant illumination of the satellite along the year and eclipses of minimum duration (Figure 3.2-3). Deviations from this condition can impact also the operation of an optical metrology between the satellites, because of the periodic interferences of the sunlight causing an increase of the photonic and thermal background on the optical bench.

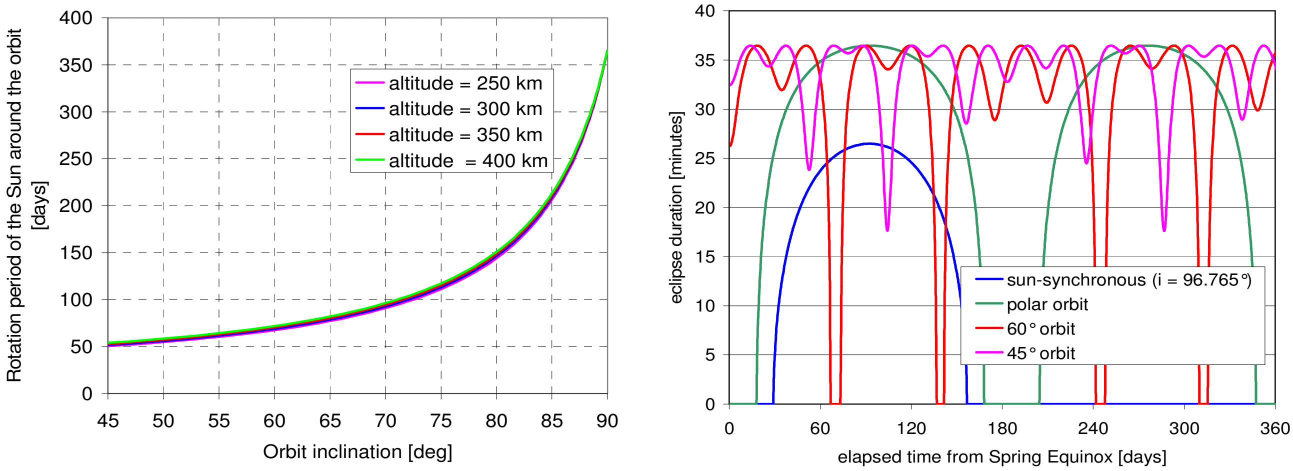

Figure 3.2-3 : Rotation period of the Sun around the orbit plane vs. inclination (left), and eclipse pattern on orbits with altitude = 325 km and different inclinations (right)

3.2.2 Number of orbiting satellites

Whereas a gravimetric mission based on gradiometry (measurement of the gravity gradient components) can be performed by a single satellite (GOCE case), for SST a minimum of two satellites is necessary. A larger number of satellites is desirable for increasing the frequency with which the whole Earth surface is covered or for measuring simultaneously more components of the gravity gradient (see e.g. the multi-satellite cartwheel formations in [RD-13]).

The satellite number has an impact on mission cost, but also on the satellite design (dimensions and mass), if the same launcher has to be shared for carrying to orbit the whole satellite fleet or part of it. For instance, VEGA cannot carry more than about 1600 kg to a sun-synchronous orbit with altitude up to 400 km. It means that, for a satellite pair launch, each satellite shall weigh strictly less than 800 kg (a margin for the dual-launch adapter shall be left). A launch of two pairs of satellites would impose a nearly prohibitive mass limit of 400 kg, in addition to sharing the volume under the launcher fairing (diameter = 2.38 m, height of the cylindrical section 3.5 m).

Thus, above a certain mass/volume limit, the number of satellites implies using more launchers (irrespective of the orbits in which the satellites are placed) or changing the launcher class.

3.2.3 Mission duration

Long duration (>5 yr) measurements of the Earth gravity are needed for resolving with sufficient accuracy the low-frequency and secular variations of the geopotential (for instance as produced by the ice cap melting in Greenland). The satellite and its resources shall be consequently designed for a long mission lifetime. Moreover, for a satellite orbiting at very low altitude, a long-duration mission implies experiencing a wide variation of the aerodynamic force. The air density at the satellite altitude is driven by the solar activity which changes cyclically with 11-year period, which is correlated the solar radio flux at 10.7 cm (F10.7) shown in Figure 3.2-4.

The influence of the solar activity on the drag force is shown in Figure 3.2-5, where a plot of the aerodynamic force on a GOCE-like satellite flying Earth pointing on a 325 km circular orbit is provided. In times of high solar activity (F10.7 = 240) the drag force is "amplified" by a factor ~7 with respect to a low solar activity (F10.7 = 60). The ratio between the maximum force at F10.7 = 240 and the minimum force at F10.7 = 60 is ~30. The situation is actually even worse, because the daily value of the solar flux (not averaged over 13 months as shown in Figure 3.2-4) can exceed 300 in periods of high solar activity. The consequence on the required thruster dynamic range is apparent and could be a technological issue for these actuators. For instance, in GOCE the dynamic range of the ion thruster is limited between ~0.6 and 20 mN, and the selection of the operational orbit altitude has been driven by this constraint. A possible countermeasure is designing the mission in accordance to a value of maximum drag, changing the altitude as needed. This however may have consequences on the gravity field resolution, which need to be addressed and traded-off.

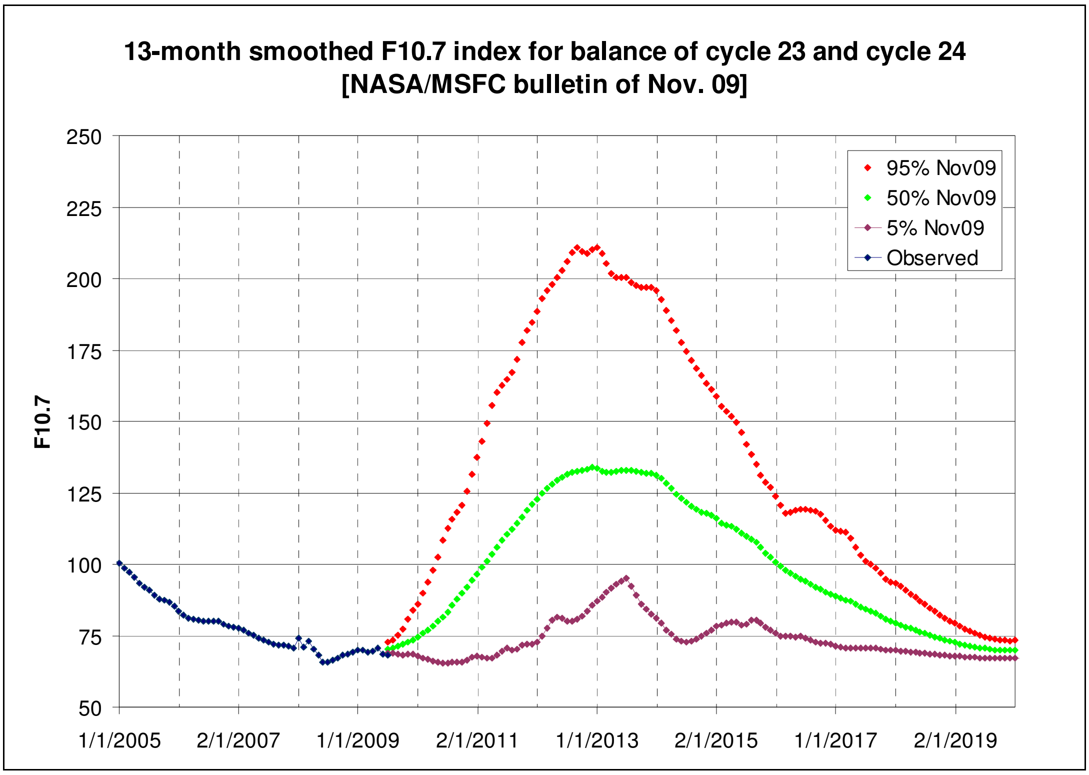

Figure 3.2-4 : Recent history and prediction of the 13-month smoothed F10.7 index [RD-14]

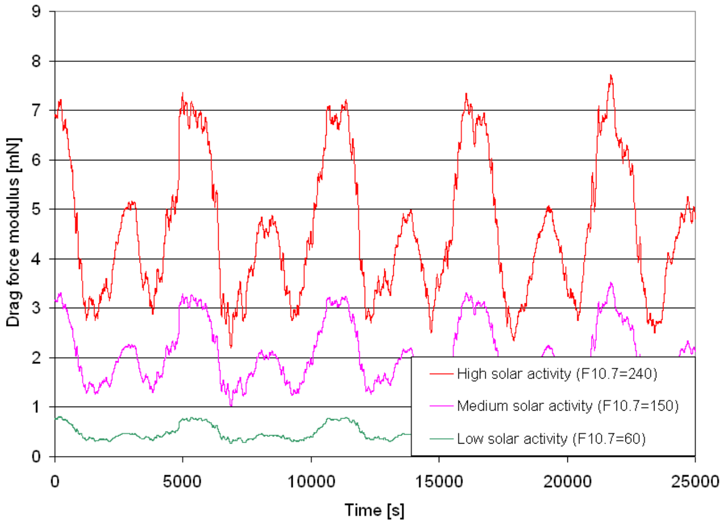

Figure 3.2-5 : Drag force on the satellite under low, medium and high solar activity [RD-14]

3.2.4 Satellite formation geometry

The SST technique can be implemented with a pair of satellites arranged in several types of formations. Figure 3.2-6 shows the basic two-satellite formations geometries: “in-line” (satellite on the same orbit, with different true anomalies, like GRACE), “pendulum” (satellites on intersecting orbits, with different inclinations or lines of nodes), “cartwheel” (satellite on intersecting orbits, with a small eccentricity, but different argument of perigee). Each formation geometry has a different effect on the sampling of the gravity field, but also on the satellite drag-free and attitude control and on the laser metrology for distance measurement.

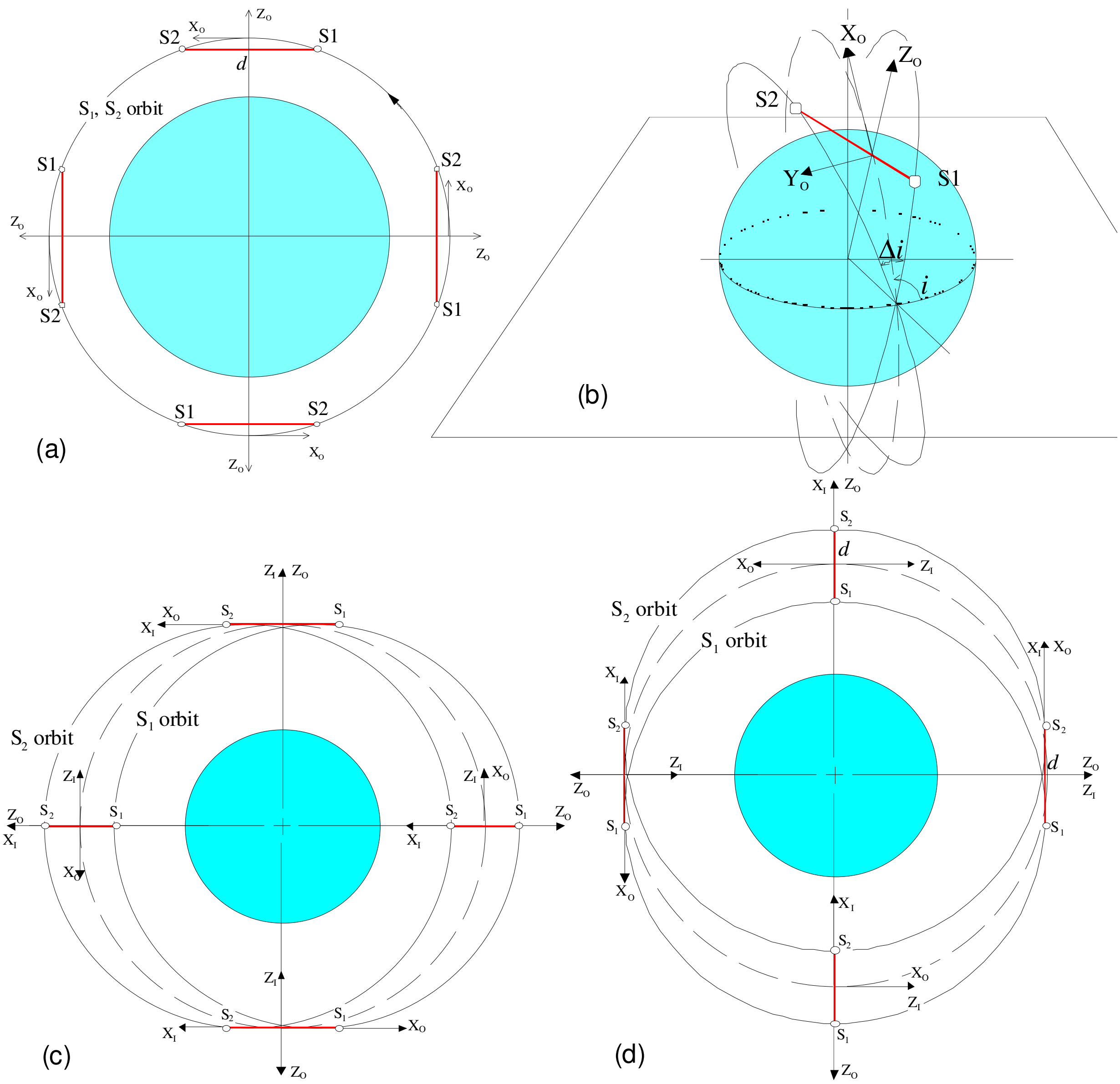

Figure 3.2-6: (a) In-line satellite formation geometry; (b) Pendulum formation geometry; (c) cartwheel formation geometry with satellite-to-satellite line aligned to the East-West direction (d) cartwheel formation with satellite-to-satellite line aligned to the North-South direction

An in-line formation is associated with an Earth-pointing attitude of the satellite. The satellite exposes always the same cross section to the main component of the drag and the main thrusters can be placed on the rear side of the satellite only. The satellite-Earth direction (i.e. the mean direction from which the electromagnetic radiation emitted or reflected by the Earth arrives to the satellite) is never aligned to satellite-to-satellite direction and therefore there is no interference between the Earth radiation and the laser metrology. The satellite-to-satellite distance changes very slowly and by a small amount around a constant mean value.

In a pendulum formation the satellite is again Earth pointing, but it must perform a cyclic yaw-steering motion phased with the orbital period in order to keep the laser beam aligned with the line joining the two satellites (or the metrology must be equipped with a mechanism enabling a large re-orientation of the beam). This satellite attitude oscillation implies that the main component of the drag force sweeps a large angular sector around the satellite and the main thrusters must be distributed around the satellite body. The satellite-to-satellite distance experiences much larger oscillations and this implies a larger dynamic range of the laser metrology and the capability to cope with a significant Doppler shift. The initial acquisition of this formation geometry (which can be obtained from the in-line formation, by applying forces to each satellite along the orbit normal, in opposite directions) requires more complex manoeuvres, time and propellant consumption with respect to the in-line case.

In a cartwheel formation the line joining the satellites keeps on average a fixed direction in inertial space (the inter-satellite line oscillates with half of the orbit period around the inertial mean direction). Each satellite must remain aligned to the inter-satellite line for keeping the laser correctly pointed (or, if the satellite keeps an Earth pointing attitude, the laser beam must be equipped with a mechanism enabling 360° rotation). The almost-inertial attitude implies that the main component of the drag force (aligned to the orbital velocity) turns once per orbit around the satellite and the main thrusters must be distributed all around the satellite body. Again, the satellite-to-satellite distance experiences large oscillations and a significant Doppler shift, with impact in the metrology dynamic range. Moreover, the inter-satellite line becomes aligned to the satellite-Earth direction twice per orbit, with potential interferences (optical and thermal) between the Earth radiation and the laser metrology.

The initial acquisition of this formation (which can be obtained from the in-line formation, by applying forces to each satellite along the orbit radius in opposite directions) requires more complex manoeuvres, time and propellant consumption with respect to the in-line case.

Last but not least, the distance between the satellites is a fundamental design driver, and not only for the laser metrology (larger distances implies higher optical powers for achieving a given signal-to-noise ratio). In fact, two satellites separated by a larger distances are subject to larger differential orbital disturbances (of gravitational and non-gravitational nature). Therefore the satellite formation is naturally more unstable and more control authority and propellant consumption is required for keeping the relative motion bounded.

3.2.5 Payload instruments for the gravity field measurement

The implementation of SST requires a metrology system for measuring the distance between the satellite COMs, as well as (at least) one accelerometer for measuring the non-gravitational accelerations of the satellite COM. Apart from the challenges imposed by the mission objectives on the design of these measurement devices, their presence on board has a significant impact on the satellite design.

A metrology of optical type, like a laser interferometer, needs reference markers (mirrors) for the distance measurement. These markers must be collocated in proximity of the COM. Thus, the satellite must be equipped with a duct that puts in communication the zone in proximity of the COM with the exterior of the satellite and vice-versa, for the passage of the laser beam. This can, in turn, have an impact on the thermal control of the inner part of the satellite (the zone of the optical bench and of the accelerometer), especially if the Sun and/or the Earth radiation periodically enter or approach the duct, depending on the orbit and/or satellite formation dynamics. The pointing of the laser beam must also follow the relative motion of the two satellites, according to the formation geometry, and this implies a coordinated action between the attitude control and the operation of a suitable laser beam pointing mechanism. An inter-satellite link is necessary to transfer the information necessary for driving the laser beam pointing system. Such a link has to be established also to exchange the absolute position, velocity and other GNSS measurements between the satellites.

The presence of accelerometer(s) on board implies that the satellite must be designed to minimize any source of disturbing acceleration (micro-vibrations, thermal “clanks”, thermo-elastic deformations, self-gravity, inductive electro-magnetic forces, etc.). Moreover, to make the most of the accelerometer performance, the satellite may have to be equipped with a drag-free control system.

3.2.6 Drag free control

Errors in the measurement of the non-gravitational acceleration arise from the coupling of the accelerometer “imperfections” with the non-gravitational accelerations themselves. For instance:

- the external acceleration is affected by the accelerometer transfer function which is characterized by a scale factor different from unity and not stable in time, and by a non-linear term as well (the so called quadratic factor);
- the acceleration which is measured along a given satellite axis contains traces of the accelerations along the other axes, due misalignments in the accelerometer mounting and non-orthogonality between the sensor axes.

The purpose of the drag free control is to reduce the external non-gravitational acceleration (in maximum value and variation) down to the limits acceptable for:

- enabling the accelerometer to operate in the finest measurement range without saturation;
- reducing the accelerometer-drag environment coupling errors below the limits established by the overall mission performance.

Of course, the action of drag-free control system depends on the atmospheric environment in which the satellite is immersed and by the requirements to be achieved. But, in any case, its implementation requires the utilization of thrusters whose force can be finely modified in a continuous manner to match the aerodynamic force acting on the satellite (at least in a given frequency band). Moreover, in general, these proportional thrusters shall be arranged in such a way as to apply forces and torques about all the satellite axes (although with different intensity), because the angular accelerations and the satellite pointing fluctuation must be precisely controlled since they play an important role too in the mission performance achievement.

3.3 Payload engineering requirements and constraints

3.3.1 Concept of ll-SST

Thanks to the much larger separation between the "proof masses", the satellites, ll-SST (Figure 3.3-1) is intrinsically more sensitive than gradiometry for measuring the time-varying gravity signal, especially at low field degrees (Figure 3.3-2). Therefore good measurement accuracy can be achieved even at the relatively high altitudes (>300 km) needed to ensure long lifetime with an affordable amount of propellant.

The fundamental observable in ll-SST (Figure 3.3-1) is the distance *variation* between two satellites produced by the gravity acceleration, Δd_G, obtained from Δd - Δd_D, where Δd is the total distance variation between the two satellites, whatever the source, as measured by a laser metrology system, and Δd_D is the distance variation produced by drag forces alone, as measured by accelerometers.

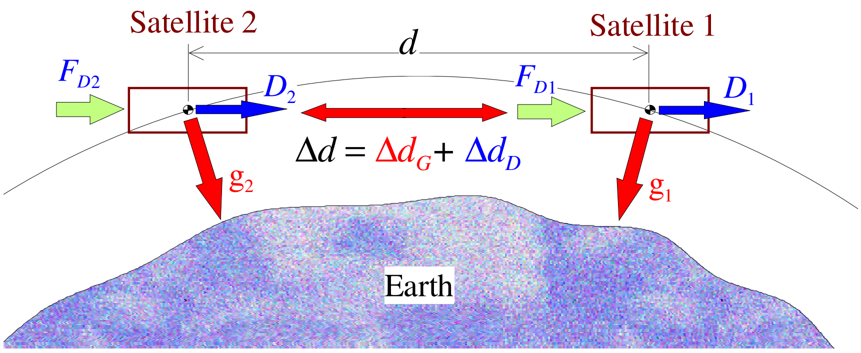

Figure 3.3-1 : Low-low satellite-to-satellite tracking concept (GRACE)

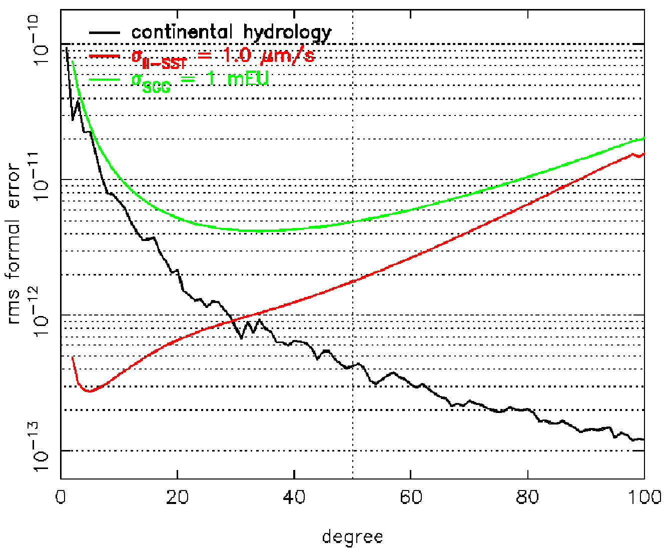

Figure 3.3-2 : Signal strength of continental hydrology compared to sensitivity of ll-SST (1 µm/s) and gradiometry (1 mE)

3.3.2 II-SST Observables

Figure 3.3-3 shows the instruments involved in the measurement of the fundamental observable Δd_G in an II-SST mission. Measurement of the total distance variation between the satellite COMs, Δd, involves three payload subsystems: (1) distance metrology, (2) angle metrology, (3) lateral displacement metrology.

1. The laser based distance metrology function performs (see Figure 3.3-4) measurement of the distance variation between the retro-reflectors (points A, C) along the optical path followed by the laser beam (A-B-C): $\Delta L = \Delta d1 + \Delta d2$.
2. The angle metrology function performs measurement of the rotation angles of Satellites 1 and 2 w.r.t. the line joining the satellite COMs ($\cong$ laser beam): $\theta1$, $\theta2$, $\psi1$, $\psi2$.
3. The lateral displacement metrology function performs measurement of the Y-Z offsets of RR2 from the laser beam axis, to ensure beam pointing.

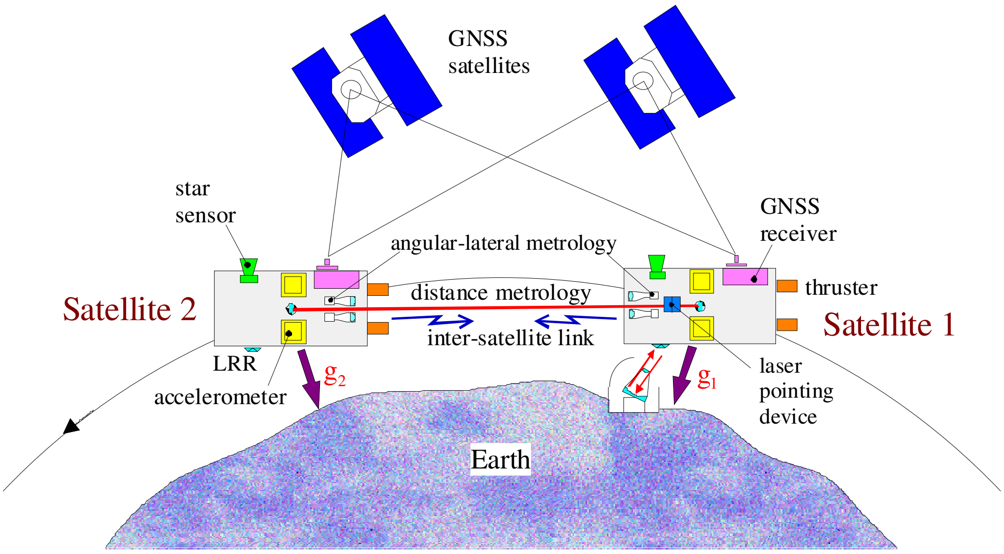

Figure 3.3-3 : Instruments involved in the measurement of the fundamental observable Δd_G in an II-SST mission

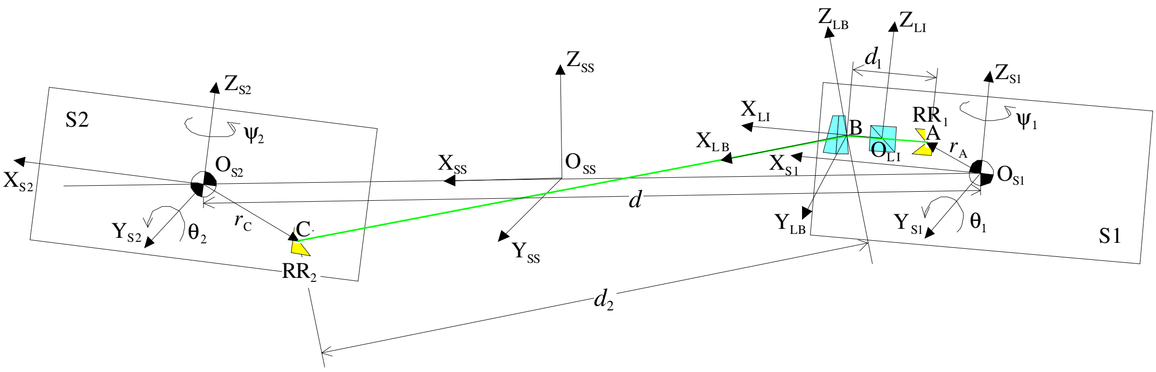

Figure 3.3-4 : Distance measurement scheme

3.3.3 Distance metrology concepts

Two versions of a heterodyne Michelson-type interferometer have been specifically designed, breadboarded and tested in view of an application to an NGGM.

Optical Transponder concept

The OT concept (Figure 3.3-5) was developed in the USA for the GRACE follow-on mission by JILA/JPL. It features a Michelson-type heterodyne interferometer based on a transceiver scheme with a master laser on Satellite 1 and a slave laser on Satellite 2, phase-locked to the former in “frequency-offset”.

The OT concept is suitable for very long distances (>100 km) thanks to its “signal regeneration” scheme. On the other hand, it requires two lasers and two interferometers operating simultaneously (extra complexity, reliability impact).

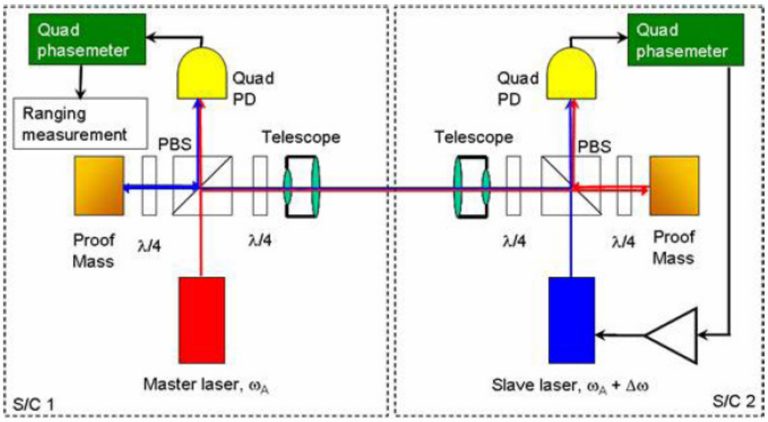

Figure 3.3-5 : Optical transponder concept

Laser retro-reflector concept

The Laser Retro-Reflector (LRR) concept (Figure 3.3-6) was proposed by TAS-I/INRIM for NGGM and has been the subject of an initial experimental development [RD-4]. It is the baseline for this study.

It features a Michelson-type heterodyne interferometer with passive retro-reflection and chopped laser beam for long-distance (> ~1 km) operation.

In the LRR concept, one laser sufficient to perform the measurement. Two lasers provide single-failure tolerance. On the minus side, the LRR is unsuitable for very long distances (> 100 km), due to the weak return optical power.

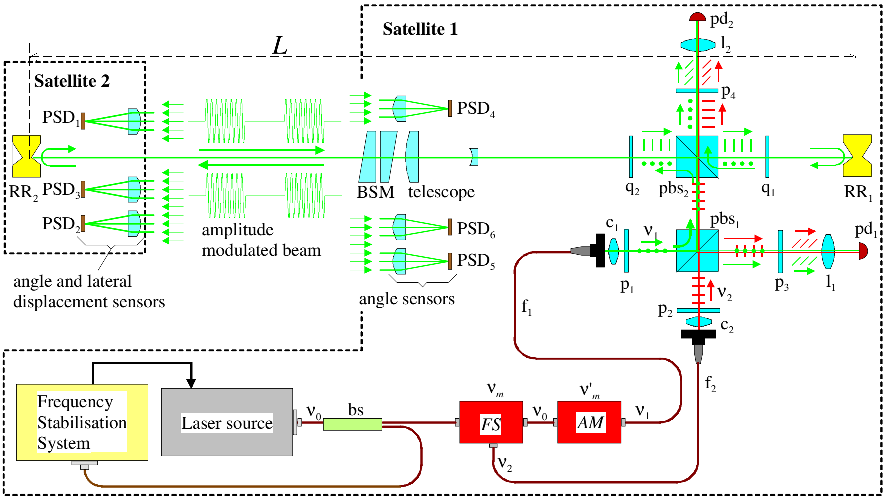

Figure 3.3-6 : Retro-reflection concept

3.3.4 Distance measurement errors and requirements

Tools for computing Δd error budgets have been developed by TAS-I, using MathCad, in the framework of [RD-5]. These tools implement analytical, but sufficiently detailed measurement models for the satellite-satellite distance and the non-gravitational accelerations, containing all the main error contributors at instrument and satellite level. The applicable measurement geometry is that shown in Figure 3.3-4. The tools can be applied to any kind of 2-satellite formation (in-line and cross-line). The error term structure and the budget inherited from [RD-5] are shown in Table 3.3-1.

Table 3.3-1 : Distance measurement error tree (values from the previous study)

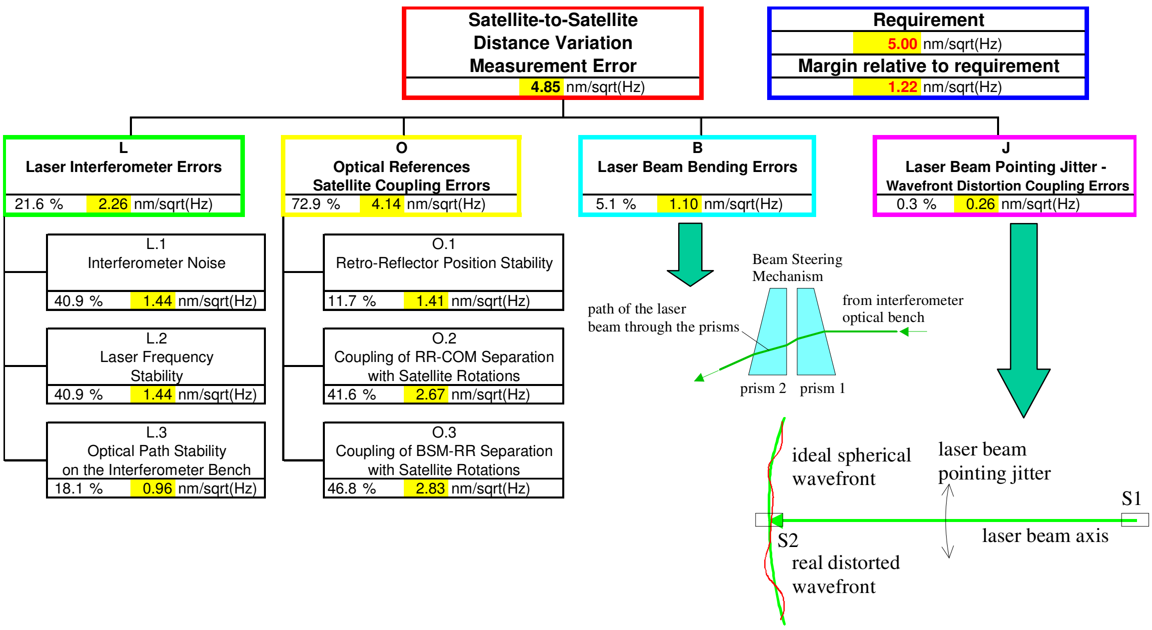

At km-length distances, the measurement performance is limited by the frequency stability of the laser source. In both interferometers developed so far (JILA/JPL, TAS-I/INRIM), a variation of the laser frequency ($\delta\nu$) produces the same effect on the measurement as a distance variation (δL): $\delta L/L = \delta\nu/\nu$.

Two techniques can be used for stabilizing the laser frequency:

- An optical resonator (or Fabry-Perot Cavity, made by two faces spherical mirrors connected by a spacer) is kept dimensionally stable by proper material choice and precise temperature control. A fraction of the laser beam is injected in the resonator and its frequency is controlled in such a way as to maintain the resonance condition (integer number of half-wavelengths contained in the resonator).
- A fraction of the laser beam is injected into a cell containing a gas (like iodine I_2) having at least an absorption line with frequency within the laser tuning range. The laser frequency is controlled so as to maximize the excitation of that absorption.

The best frequency stabilization performance achieved in the laboratory by these techniques on an Nd:YAG laser (λ = 1064 nm) in the bandwidth of interest for an NGGM (1 ÷ 100 mHz) is $\delta\nu/\nu \cong 10^{-13}$ Hz$^{-1/2}$ ($\delta\nu \cong 30$ Hz/√Hz); see Figure 3.3-7. Therefore, the distance measurement noise limit (for negligible intrinsic noise of the interferometer) is $\delta L \cong 10^{-13} L$ Hz$^{-1/2}$, i.e., about 1 nm·Hz$^{-1/2}$ at 10 km, about 10 nm·Hz$^{-1/2}$ at 100 km, and so on.

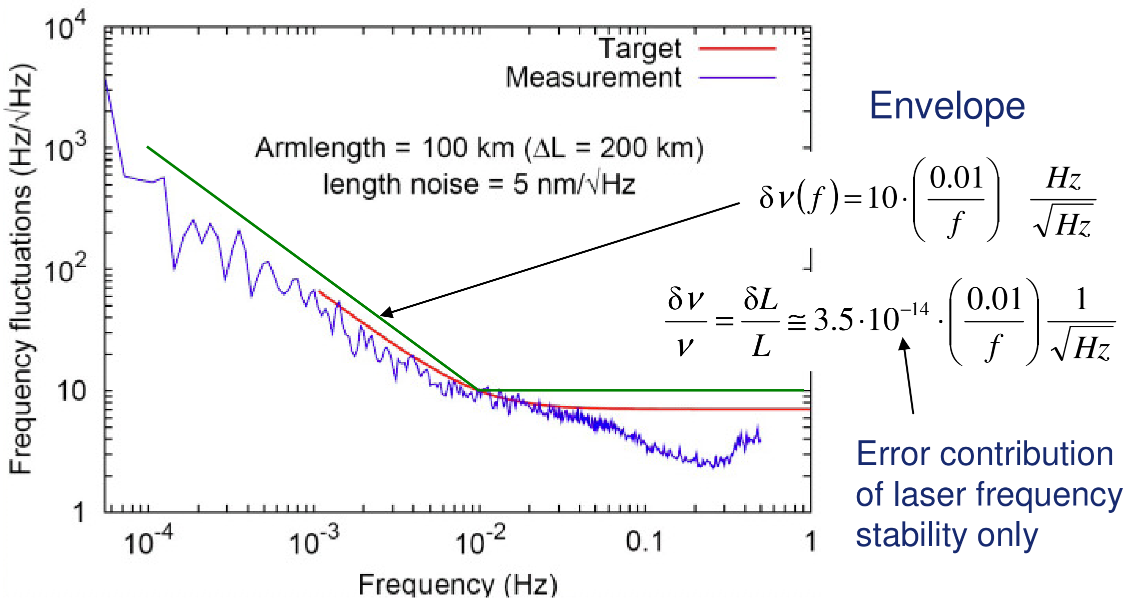

Figure 3.3-7 : Best frequency stability achieved in laboratory using a reference cavity [Ref. G. Heinzel, "LISA technology for gravity-field missions", Graz Workshop, 30/9 2009]

As in [RD-5], we propose to take as performance objective (assumed best performance achievable in orbit) an envelope about 10 times worse than the best lab performance shown above (taking also into account that the laser frequency stability is only one of many contributors to the final performance, as shown in Table 3.3-1):

$$\frac{\delta d}{d} = \begin{cases} 5 \cdot 10^{-13} \cdot \left(\frac{0.01}{f}\right) \frac{1}{\sqrt{Hz}}, & f < 0.01\, Hz \\ 5 \cdot 10^{-13}, & f \geq 0.01\, Hz \end{cases}$$

This envelope is shown in Figure 3.3-8 as both fractional error and distance error.

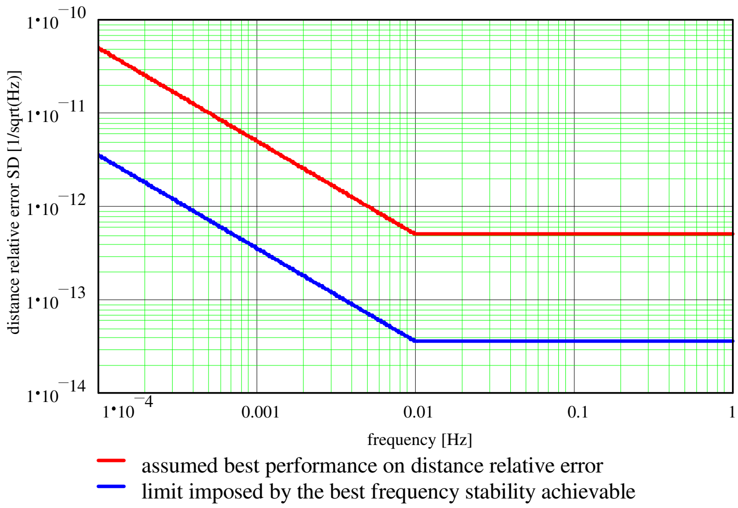

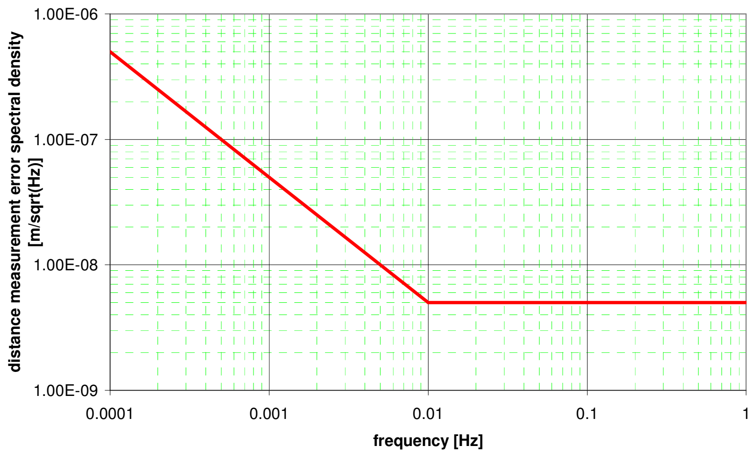

Figure 3.3-8 : (top) Assumed best performance achievable in orbit on the COM-COM distance d overall relative error; (bottom) corresponding requirement on distance measurement error Δd, for d = 10 km

3.3.5 *Ancillary distance metrology requirements*

Angle metrology

Measurement of the S1, S2 rotation angles w.r.t. the line joining the satellite COMs (≅ laser beam): θ_i, ψ_i

- measurement range: ±1 °
- maximum measurement error $\leq 10^{-4}$ rad
- measurement error spectral density as shown in Figure 3.3-9.

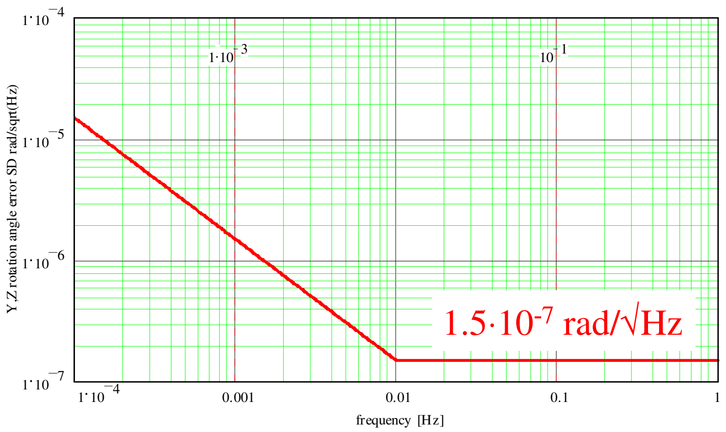

Figure 3.3-9 : Angle metrology performance

Lateral displacement metrology

Measurement of the laser beam axis lateral displacements relative to the retro-reflector on S2, such as to ensure a laser beam pointing control with maximum error $\leq 10^{-5}$ rad (≤0.1 m at 10 km). The corresponding pointing stability spectral density requirement is shown in Figure 3.3-10.

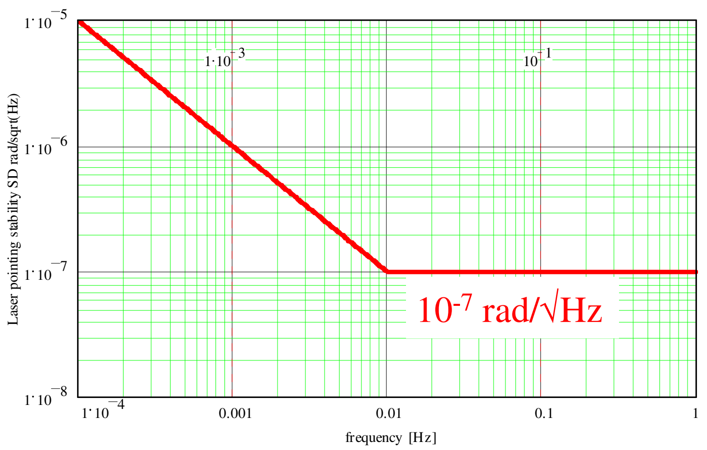

Figure 3.3-10 : Laser beam pointing stability performance

3.3.6 Resources needed by the distance measurement system

A preliminary assessment of the s/c resources/services required by the distance measurement system (distance, angle, lateral metrology) is shown in Table 3.3-2.

Table 3.3-2 : Distance measurement system resources

Item	Value	Remarks
Mass	60 kg	including optical bench
Power demand	100 W	
Telemetry generation rate	1.5 kbps	distance + angle metrology; data output at 10 Hz
Inter-satellite telemetry rate	3 kbps	lateral metrology on S2; data output at 100 Hz
On board processing power	~20,000 flops	mainly on S1 for distance metrology + beam pointing management. Large amount of the computation on the distance metrology and angle/lateral metrology shall be performed by a dedicated FPGA/ ASIC
	~10000 flops	required by the pointing control
Absolute / Relative Pointing Error	TBD	not very demanding if the laser beam pointing function is performed by a dedicated device and not by the S/C
Relative velocity control	<15.9 m/s	limited by the heterodyne frequency
Relative acceleration control	<120 m/s²	limited by the laser beam chopping scheme
Temperature stability	TBD	stable temperature required on the optical bench and in the optical cavity utilized for the laser frequency stability

Note on the optical power

The output optical power of the laser source was set = 0.75 W in the previous NGGM study [RD-5]. Figure 3.3-11 shows the optical power received by the laser interferometer (after retro-reflection) vs. the inter-satellite distance, compared with the minimum power requirement, in the following cases:

- Case 1: same distance measurement error (δd = 5 nm/√Hz);
- Case 2: same relative measurement error $\delta d/d = 5 \cdot 10^{-13}$ 1/√Hz) whatever the distance.

The optical power requirement is fulfilled up to ~85 km in Case 1 and up to >100 km in Case 2. We conclude that the distance metrology based on the retro-reflector is anyway limited by the laser frequency stability ($\nu\delta/\nu = \delta L/L$) and not by the optical power.

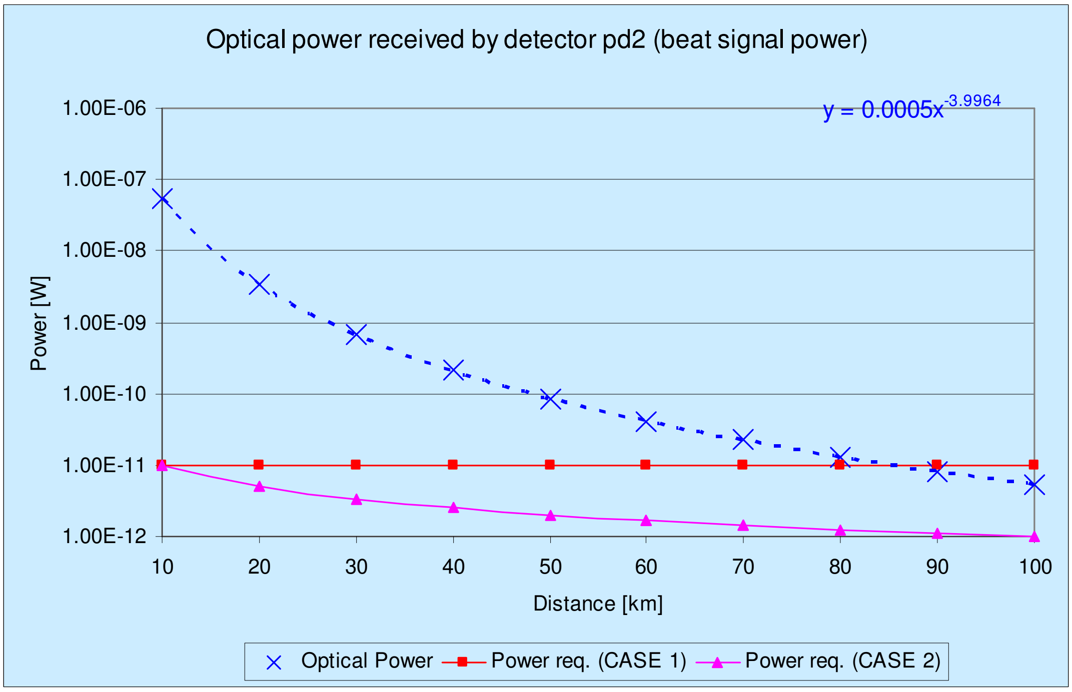

Figure 3.3-11 : Optical power received by the laser interferometer (after the retro-reflection) vs. inter-satellite distance, compared with minimum power requirement in Case 1, 2.

3.3.7 Alternative implementation options of the distance measurement system

3.3.7.1 Distance metrology without laser frequency stabilization

The frequency stabilization system has a significant cost (~2x) and complexity impact (frequency reference, closed loop control) on the distance measurement system. Therefore the question arises of whether the frequency stabilization can be avoided, while still realizing an improvement w.r.t. the k-band RF metrology of GRACE.

Figure 3.3-12 shows a record of laser stability performance achieved in the lab. The blue line on top represents a free-running laser. The same line is translated into a distance variation measurement error (for d = 10 km) in Figure 3.3-13. We conclude that the free running laser cannot improve the GRACE measurement performance. Therefore the laser stabilization system cannot be avoided.

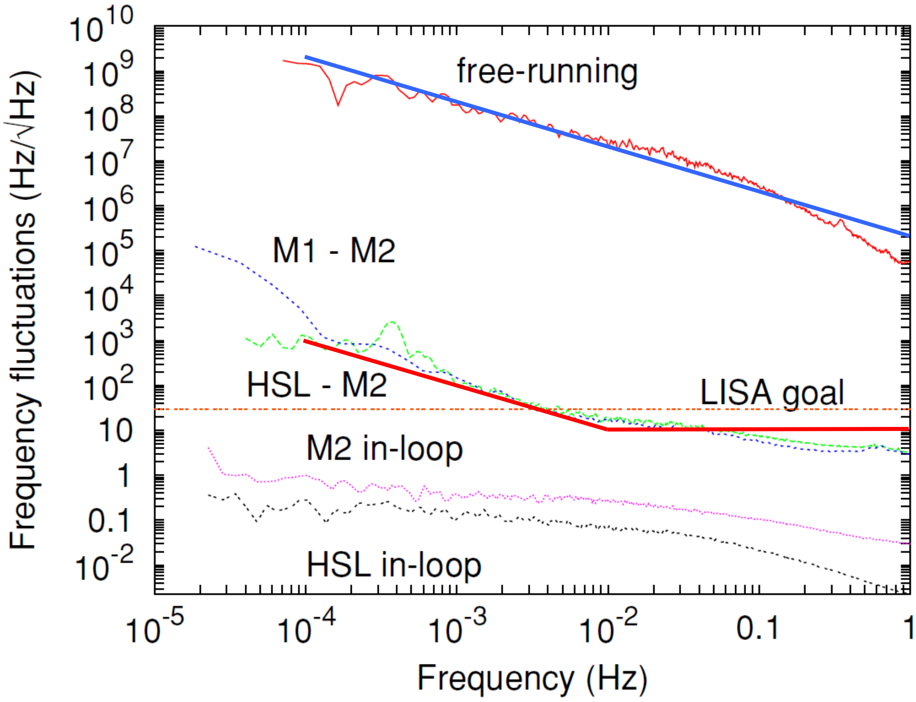

Figure 3.3-12 : Laser frequency stability performance (M. Tröbs et al., Laser development for LISA, Class. Quantum Grav. 23 (2006) S151–S158)

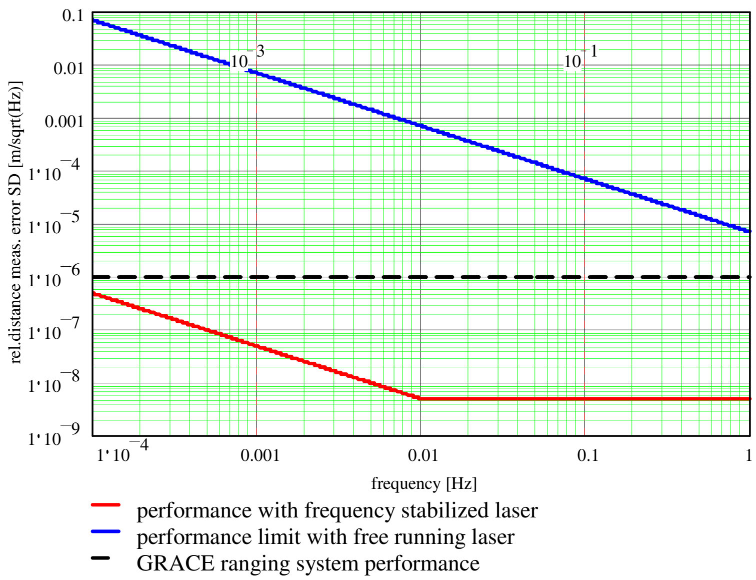

Figure 3.3-13 : Distance variation measurement error computed for d = 10 km

3.3.7.2 *Laser beam pointing performed by the S/C attitude control*

The advantages of a dedicated laser beam pointing device consist in:

- relaxed attitude control requirements;
- satellite attitude control decoupled from the relative motion of the satellites.

The drawbacks include

- more complexity and less reliability (continuously operating mechanism required);
- disturbances induced on the distance measurement and, potentially, on the accelerometers.

The laser beam pointing task may be transferred to the S/C attitude control on condition that:

- the current requirements on laser beam pointing and stability (10^{-5} rad, 10^{-7} rad/√Hz) are relaxed by a factor of about 10 (TBC);
- the attitude motion induced by the tracking of Satellite 2 is shown compatible with the attitude stability requirements.

This option will be further addressed in the study.

3.3.7.3 *Dedicated angle metrology replaced by S/C equipment (GPS, star trackers)*

In principle, the satellite rotation angles w.r.t. the line joining the satellites can be obtained by using:

- the satellite absolute and relative position provided by GPS, from which the inertial orientation of the satellite-to-satellite line can be reconstructed;
- the inertial attitude of each satellite provided by the star trackers.

The angle metrology may be replaced by GPS and star trackers on condition that:

- the measurement error spectral density (set to $1.5{\cdot}10^{-7}$ rad/√Hz in the previous NGGM study) is relaxed by at least one order of magnitude (TBC);
- possibly, the laser beam divergence (currently 10^{-4} rad) is increased.

If the beam pointing device is removed (and therefore there is no bending of the laser beam outgoing/incoming from/to S1), the nearly constant rotation angles of S1 relative to the beam (≡ satellite-to-satellite line) could be measured using a quadrant photodiode in the laser interferometer (same concept as the GRACE-follow-on metrology).

This option will be further addressed in the study.

3.3.8 Non-gravitational acceleration measurement errors and requirements

The objective is measuring the non-gravitational differential acceleration of the two satellites along the line joining the COMs (Figure 3.3-14):

$$D_1 - D_2 = \Delta\ddot{d}_D \Rightarrow \Delta d_D = \iint \Delta\ddot{d}_D dt$$

To this purpose, the payload includes accelerometers and dedicated angle metrology. The accelerometers measure the linear non-gravitational acceleration of the COM of each satellite, $\underline{D}_1$ and $\underline{D}_2$, in the Satellite Reference Frame.

The angle metrology measures the rotation angles of Satellite 1/2 Reference Frames w.r.t. the line joining the satellite COMs: θ_1, θ_2, ψ_1, ψ_2.

The error budget inherited from [RD-5] is shown in Table 3.3-3.

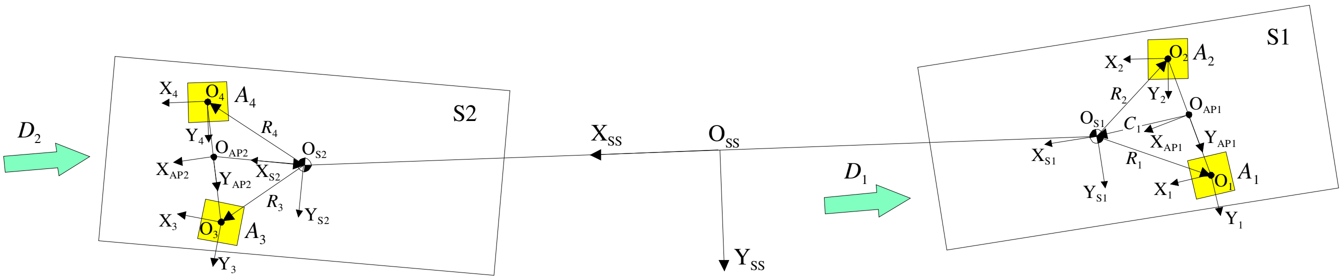

Figure 3.3-14 : Non-gravitational acceleration measurement scheme

Table 3.3-3 : Non gravitational acceleration measurement error tree (values from the previous study)

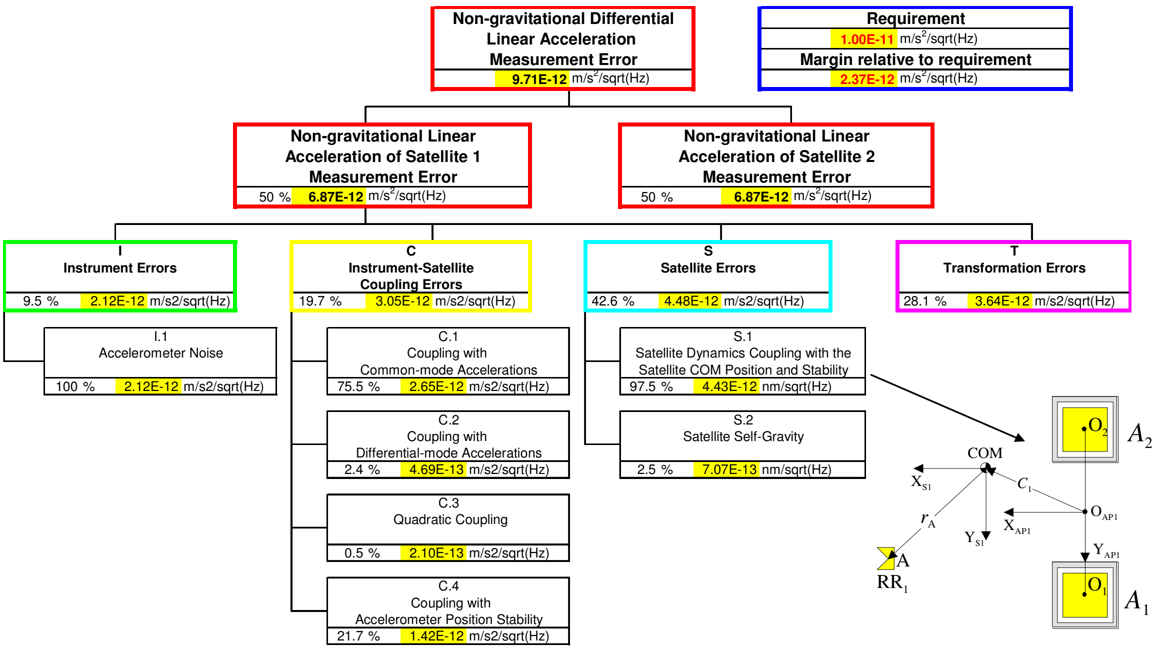

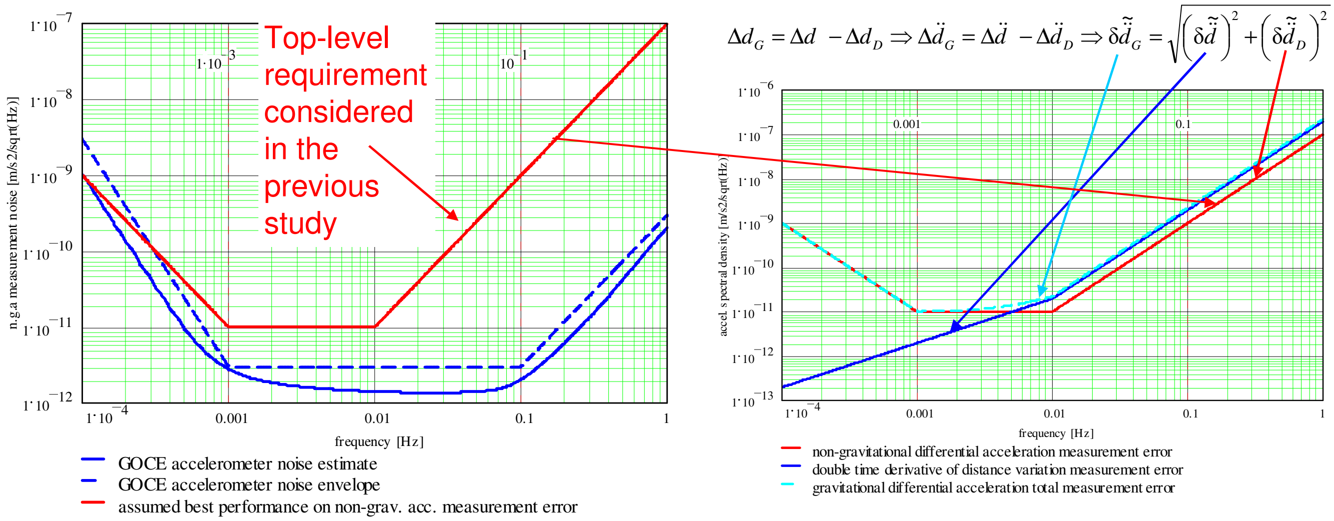

Figure 3.3-15 : (left) GOCE accelerometer noise along the ultra-sensitive axes considered as ultimate performance limit (note GRACE acceleration noise = 10^{-10} m/s²/√Hz); (right) Non-gravitational acceleration noise increase at high frequency matched to the double time derivative of the distance variation measurement noise.

The ultimate limiting factor of the acceleration measurement is the accelerometer intrinsic noise. Figure 3.3-15 (left panel) shows the GOCE accelerometer noise mask along the ultra-sensitive axes, considered as the ultimate performance limit, and the performance requirement assumed in [RD-5]. The latter, in turn, is matched, at the high frequency end, to the double time derivative of the distance variation measurement noise from the ll-SST (same figure, right panel). This prescription realizes an improvement of a factor of 10 w.r.t. the GRACE performance (acceleration noise=10^{-10} m/s²/√Hz).

3.3.9 Ancillary acceleration measurement requirements

As shown in Table 3.3-3, the acceleration error budget includes a transformation error which depends on the measurement of angles. The corresponding requirements are:

- Satellite misalignment in the Satellite-Satellite Reference Frame (SSRF): θ_P, $\psi_P \leq 1°$
- Rotation angle measurement error: $\delta\theta_P$, $\delta\psi_P \leq 10^{-4}$ rad
- Envelope of satellite pointing requirements from distance variation measurement and non-gravitational acceleration measurement: θ, $\psi \leq 1°$, $\delta\theta$, $\delta\psi \leq 10^{-4}$ rad.

Figure 3.3-16 shows the corresponding requirements in the frequency domain (again, envelope of pointing requirements from distance variation measurement and non-gravitational acceleration measurement).

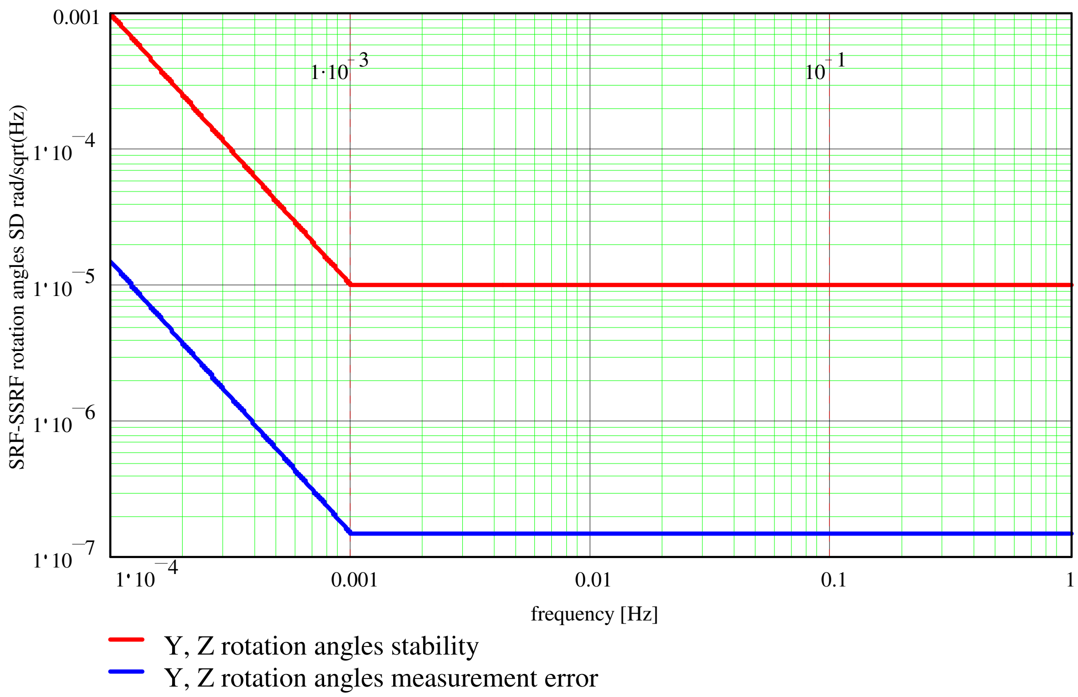

Figure 3.3-16 : Angle metrology requirements (red: satellite rotations stability requirements; blue: satellite rotation measurement error requirements)

3.3.10 Resources needed by the acceleration measurement system

A preliminary assessment of the s/c resources/services required by the acceleration measurement system is shown in Table 3.3-4.

Table 3.3-4 : Acceleration measurement system resources

Item	Value	Remarks
Mass	22 kg	two GOCE-like accelerometers per S/C assumed
Power demand	35 W	
Telemetry generation rate	3 kbps	3 linear + 3 angular accelerations per accelerometer; data output at 10 Hz
Linear acceleration control	$\leq 1 \cdot 10^{-6}$ m/s²	Maximum value. Requirement on residual linear acceleration spectral density shown in Figure 3.3-17.
Angular acceleration control	$\leq 1 \cdot 10^{-6}$ rad/s²	Maximum value. Requirement on residual angular acceleration spectral density shown in Figure 3.3-18

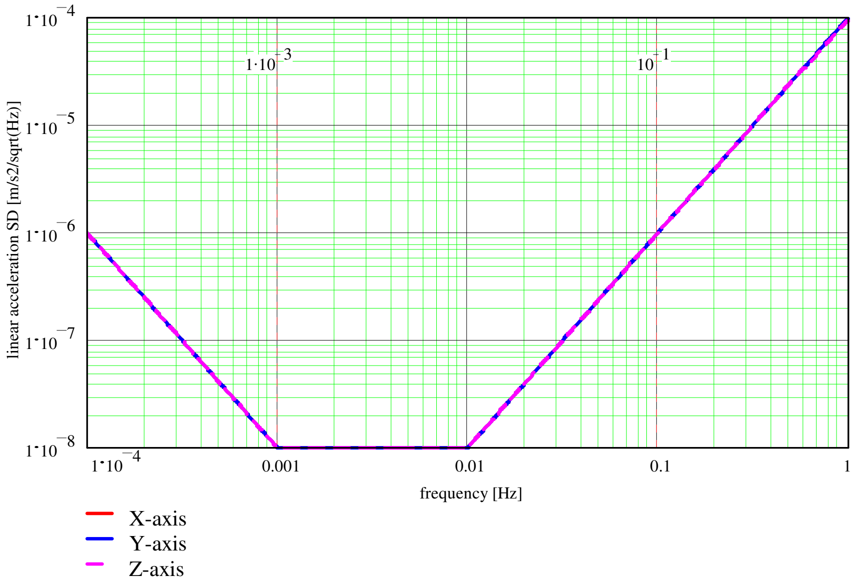

Figure 3.3-17 : Residual linear acceleration spectral density limit (control requirement)

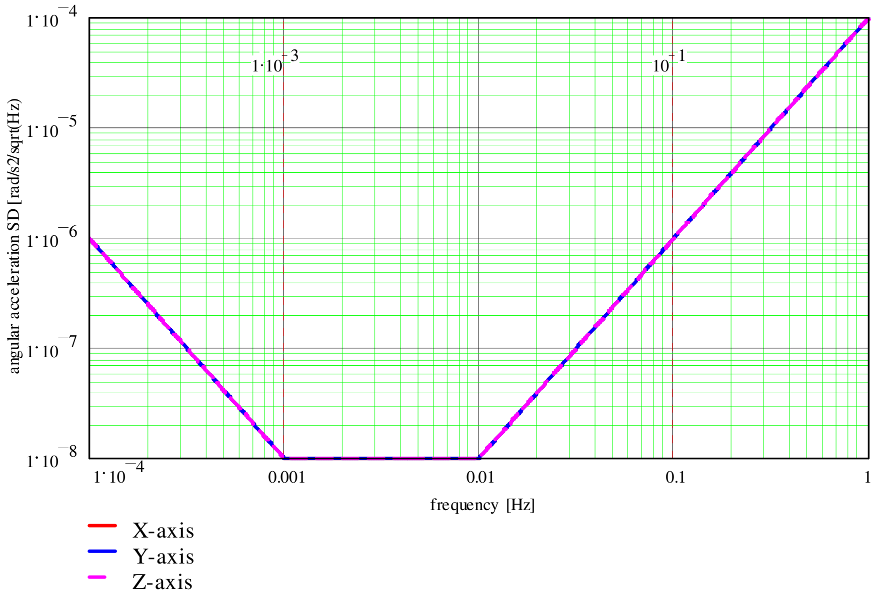

Figure 3.3-18 : Residual angular acceleration spectral density limit (control requirement)

3.3.11 *Alternative implementation options of the acceleration measurement system*

3.3.11.1 S/C without drag-free control

Figure 3.3-19 shows an example of the accelerations being measured by GOCE in flight, with and without the drag free control.

With a factor of ~10 relaxation of the residual linear acceleration requirements, the drag control in the radial and cross-track directions could be avoided (with a benefit for thruster dynamic range), whereas in-track control still seems necessary (TBC by further disturbance and performance analysis).

Better attitude control than in GOCE (±3 to 4º in yaw) is necessary to guarantee the optical link, even if a dedicated device is used for laser beam pointing. Electric thrusters are the candidate actuators, since reaction wheels are too noisy for the accelerometers.

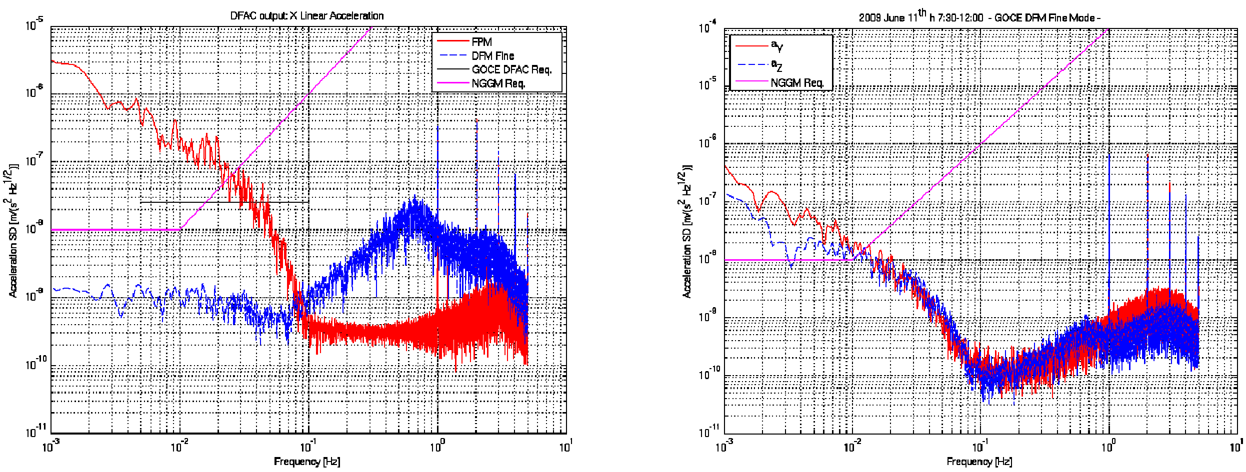

Figure 3.3-19 : GOCE measured accelerations with and without drag free control (~255 km, low solar activity)

3.4 Satellite platform drivers

The identified mission design parameters affecting the satellite platform include:

- Launcher type and number of launches
- Physical configuration (mass, volume, shape)
- Structure design and Thermal Control complexity
- Electrical power system design (solar array efficiency, power system density)
- On board data handling (science data rates, ancillary data rates, mass memory size, on board processing power)
- Telecommunications (telemetry rates to ground station, frequency of contacts with ground station, inter-satellite data exchange)
- Orbit control (orbit maintenance needs, frequency, propellant budgets)
- Attitude & drag free control (pointing accuracy, laser pointing control, linear and angular acceleration control)
- Relative satellite motion (relative range control accuracy, formation keeping).

The review below will be made with reference to the known designs of GOCE [RD-10] and GRACE [RD-11], working out and discussing the design upgrades that will be needed for an SST mission with laser metrology that we will call “GRACE+”. The GOCE and GRACE design parameters are in Table 3.4-1.

Table 3.4-1 : GOCE and GRACE design parameters [RD-10] [RD-11]

Parameter	GOCE	GRACE
On-orbit design life [yr]	2.4	5
Initial orbit altitude [km]	260	500
Orbit maintenance strategy	Constant-h	Free decay
Orbit inclination [deg]	97	89
Payload mass [kg]	195	22
Propellant mass [kg]	54	29
Bus dry mass [kg]	812	331
Total s/c dry mass [kg]	1007	353
Total s/c wet mass [kg]	1061	382
Payload dry mass fraction [%]	19.3%	6.2%
S/c volume [m^3]	5.83	1.96
S/c dry density [kg/m^3]	173	180
Launch vehicle	Eurokot	Cosmos
Stabilization type	3-axis	3-axis
Number of real-time controlled degrees of freedom (attitude + orbit)	4	4
Bus Pointing Accuracy [deg]	3	0.05
Bus Pointing Knowledge [deg]	0.03	0.008
Range Measurement Accuracy [$m/Hz^{-1/2}$]	n.a.	8.0E-06
Acceleration Control Accuracy [1e-12 $m/s^2/Hz^{-1/2}$]	1	n.a.
Propellant type	Xenon (N for calibration)	N
Number of thrusters	2	16
Structure mass [kg]	348	191
Structure mass ratio	33%	50%
Thermal control mass [kg]	29	13
Thermal control dry mass ratio	2.9%	3.7%
Power system mass [kg]	137	107
Battery type	Li-ion	NiH2
Solar cell type	GaAs	Si
Solar array area [m^2]	8.5	4.8
Solar array efficiency BOL [W/m^2]	148	33
Solar array mount	body	body
Power production BOL [W]	1260	160
Power demand EOL [W]	1025	122
Power demand average [W]	1020	122
Power system density [W/kg]	7.4	1.1
Power system mass fraction at launch	13.0%	28.0%
Comms band	S	S
Telemetry generation rate [kbit/s]	14	16
Telemetry data rate [kbit/s]	1200	1000
Transmit power [W]	0.25	2
On board Processing power [MIPS]	17	5 (estimate)
Mass memory size [Mbit]	8,000	1400
Harness mass [kg]	77	20
Harness dry mass fraction [%]	7.6%	5.7%
Lines of SW code [k lines]	320	30 (estimate)

3.4.1 Launcher

For cost reasons, “small” launchers only will be taken into consideration. The candidates are Vega and Rokot; Soyuz-Fregat might be taken into consideration for multiple launches (2 satellite pairs). Table 3.4-2 shows some typical performance data. Vega and Rokot are essentially equivalent; Soyuz provides approx. 1.5 to 3 times the volume and mass performance at twice the cost. The launch mass performance in SSO is typical for all circular LEOs, with some extra mass available if the inclination is polar or less than polar (see Figure 3.4-1).

Table 3.4-2 : Performance data of ESA small launchers

Launcher	Fairing Diameter [mm]	Mass into SSO [kg]	Cost [M€]
Vega	2380	1500 kg (700 km)	22
Rokot	2100 - 2380	1250 kg (280 km)	20
Soyuz-Fregat 2B	3800	4900 kg (660 km)	45

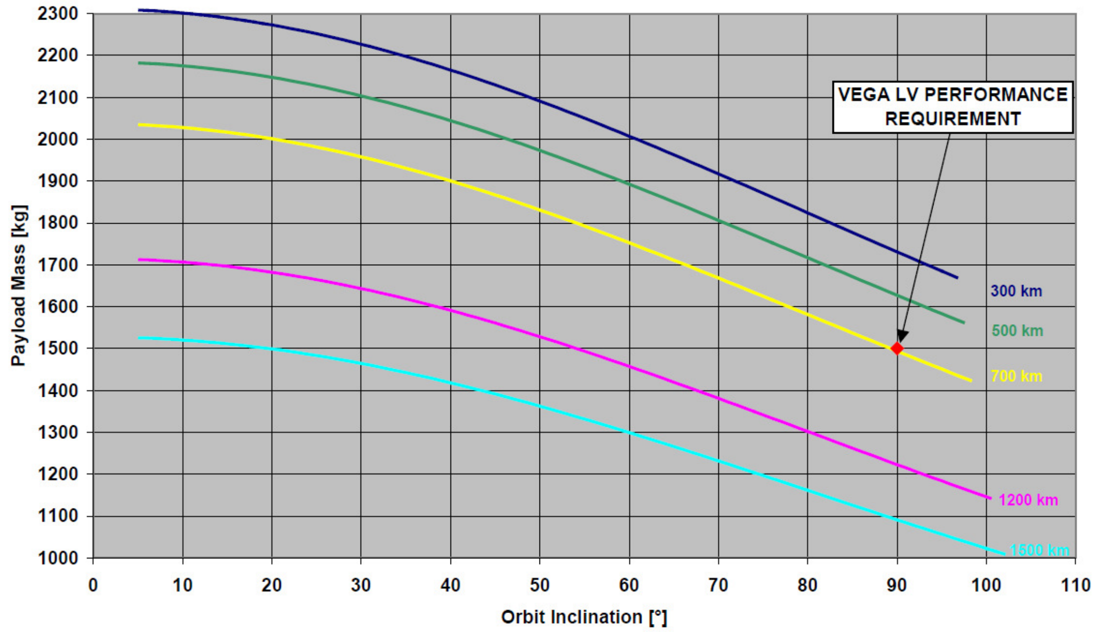

Figure 3.4-1 : Vega launch vehicle performance for circular orbits

3.4.2 Orbit Maintenance

A crucial feature of the NGGM is whether the orbit altitude is maintained, or not. In GOCE, orbit maintenance is implemented as a by-product of the drag free control. In GRACE, the altitude is left to decay freely. There are two major disadvantages to a freely decaying orbit:

- reduced magnitude of the gravity signal: to grant a long lifetime, the initial altitude must be high. In normal circumstances, most of the satellite lifetime will be spent at the higher end of the selected altitude range;
- continuously varying monthly ground track pattern: as the altitude changes, the satellite will continuously cross orbital resonances, occasionally leading to severe loss of resolution (Figure 3.4-2).

To find the characteristics of the time-varying gravity, the gravity field will be solved for on a monthly basis, as in GRACE, or possibly on an even shorter time basis. The changing altitudes and ground track patterns would affect both the space resolution and the time resolution of the gravity field solutions. It seems reasonable to conclude that the NGGM orbit will be actively maintained.

In a long duration mission, the means of orbit maintenance can only be high-specific-impulse thrusters with thrust levels in the range of tens of mN (Figure 3.4-3), i.e., ion thrusters. Table 3.4-3 shows that the propellant needed to maintain the orbit of a 500-kg satellite for 6 years is on the order of a few percent of the satellite mass, under the assumption of 3000s specific impulse. With conventional hydrazine propulsion, the propellant fraction would exceed 1/3 of the satellite mass.

Even when flying at constant altitude, across a time span of several years the changing phase of the solar cycle will cause a large variation of the drag force. This will have an impact on the propellant consumption as well as on the dynamic range requirement of the thrusters. For this reason, the operational orbit altitude may be adjusted from time to time according to the solar activity, so as to maintain near-constant drag conditions. As an alternative, especially for constellation geometries that do not minimize the drag cross section all along the orbit, operational constraints might be imposed in times of high solar flux.

Constellations which do not share the same orbital plane have an additional maintenance cost. For example, in an N-S (or E-W) constrained cartwheel, the line of apsides of the two orbits must be kept in the N-S (E-W) inertial direction. In a polar orbit at 312 km altitude, the argument of perigee drifts by -4.2°/day. The compensation ΔV is 0.28 m/s/day, leading to 10.5 kg propellant over a 6-yr mission (under the same assumptions as above). This propellant mass budget is comparable to the drag-induced orbit maintenance calculated above. Again, the mass penalty could not be afforded if conventional propulsion were used.

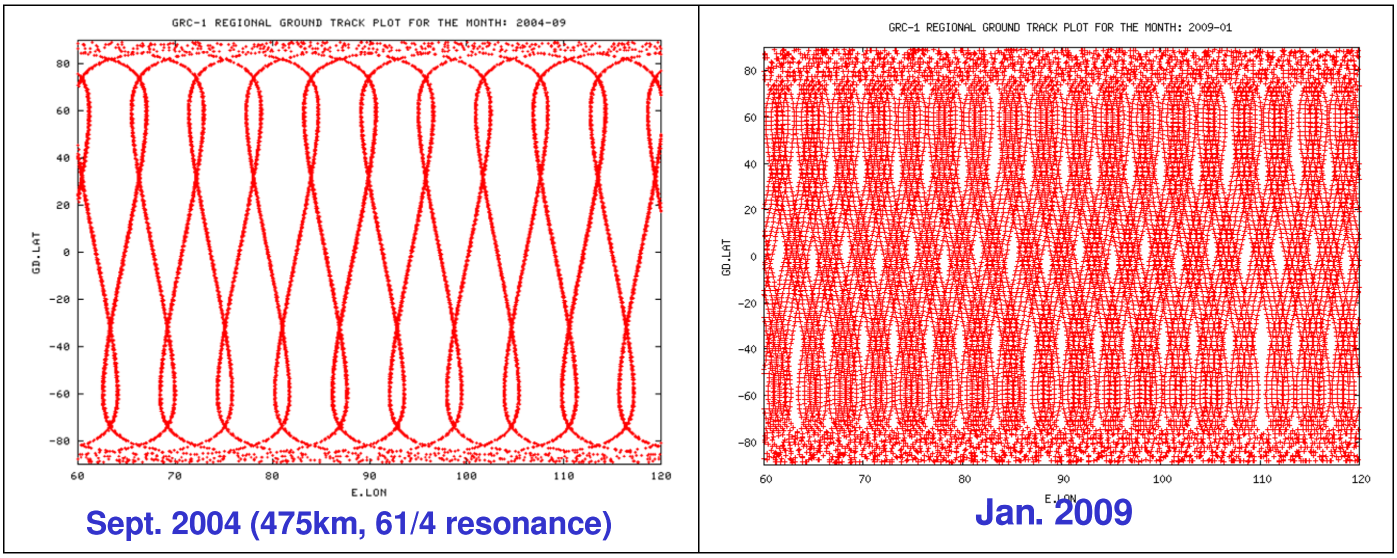

Source: http:// www.csr. utexas.edu/grace/operations/gtrk_mons

Figure 3.4-2 : Examples of widely varying GRACE ground track patterns

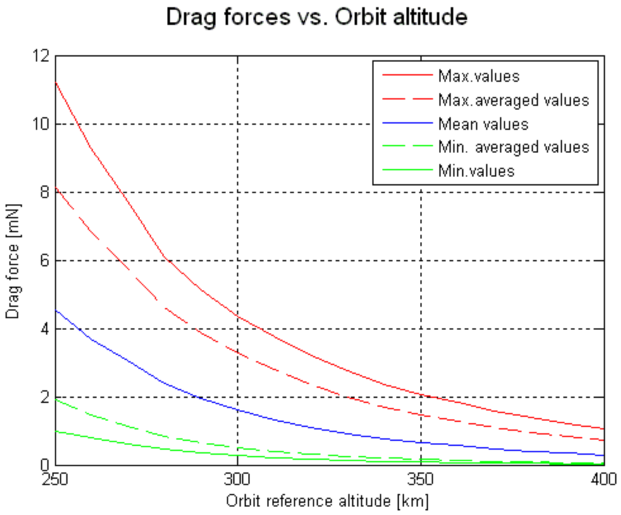

Figure 3.4-3 : Example of range of variation of the drag force as function of orbit altitude. Sun-synchronous orbit, area-to-mass ratio = 10^{-3} m²/kg, NASA solar flux forecast of Jan. 2009

Altitude [km]	Fmin / average [mN]	Mp [kg]	% Msat
250	2	26	5%
300	1	13	3%
350	1	13	3%
400	1	13	3%

Altitude [km]	Fmax / average [mN]	Mp [kg]	% Msat
250	8	103	21%
300	3.5	45	9%
350	1.5	19	4%
400	1	13	3%

Table 3.4-3 : Propellant mass for a 6-year mission under the min-averaged and max-averaged conditions of Fig. 3.4-3 (500-kg satellite, 3000s specific impulse)

3.4.3 Physical Configuration, Structure and Thermal Control

The physical configurations of GOCE and GRACE have numerous common features, driven by the low-altitude orbits, the requirement to minimize surface forces and torques, and the payload sensor requirements. These drivers include:

- long and slender shape, the external shell as load-carrying structure, leading to uncommonly high structure mass ratios (GOCE: 33%; GRACE: 50%).
- Symmetry, aerodynamic shape
- accurate CoM positioning requirement, leading to considerable balance mass allocated (GOCE: 60 kg; GRACE: 35 kg)
- Shape stability requirements under thermal loads.

It is interesting to note that neither GRACE nor GOCE have been strongly driven by launch mass requirements. This comfortable mass margin status must have helped meeting the above requirements.

In GOCE, the sun-synchronous orbit greatly facilitated the thermal design (one face permanently in shadow, small range of variation of the solar aspect angle of the satellite surfaces). This advantage did not apply for GRACE, which however had very small power needs and very low power dissipation.

A GRACE-like satellite pair with mutual laser ranging will continue to be driven by the aspects mentioned above (high structure mass ratio, aerodynamics, CoM, thermoelastics). In addition, mass and volume constraints (e.g. from twin launch on Rokot), power demand (laser system & ion thrusters), and radiating surfaces, will be much more demanding and may become limiting factors (see also the considerations about power in the next chapter).

Figure 3.4-4 shows an accommodation concept of two GOCE-like prism-shaped satellites in the Vega fairing. The front cross section (1.1m^2) is the same as GOCE, the volume is reduced by about 20%; the room available for solar arrays is strongly constrained.

Constellations in which the mutual laser LoS is not in the direction of the velocity (e.g. cartwheel, pendulum…) face additional configuration constraints. In high-inclination orbits such as those needed for wide latitude coverage, the air density changes by factor of 3 from equator to poles. A prism-shaped satellite may minimize the variation of the drag force by matching the surface area ratio to the density ratio, resulting in an additional configuration constraint (Figure 3.4-6).

In pendulum and cartwheel constellations, the drag force rotating around the body suggests the shape of a flat cylinder as a convenient solution (Figure 3.4-7). Again, this gives rise to further configuration constraints. In the pendulum (Figure 3.4-7, left), the drag force scans a ≈45° angular sector around the satellite once per orbit; a cylindrical satellite with the long axis aligned to the local vertical always offers same cross section to drag. In the cartwheel (Figure 3.4 5, right), the drag force turns around the satellite body once per orbit; again, a cylindrical satellite, now with the long axis aligned to the orbit normal, always offers same cross section to drag. If this cross sectional area is chosen to be as small as the cross section of GOCE (1.1m^2), a very strong volume constraint arises (Figure 3.4-5).

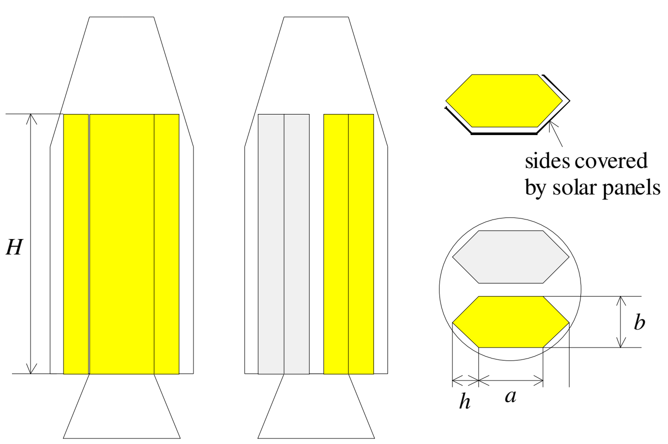

Launcher constraints (Vega): Front cross section: 1.1 m²; lateral cross sections: 7.2 m² and 3.2 m²; Volume: 4.48 m³

Figure 3.4-4 : Accommodation of two prism-shaped satellites in the launcher fairing

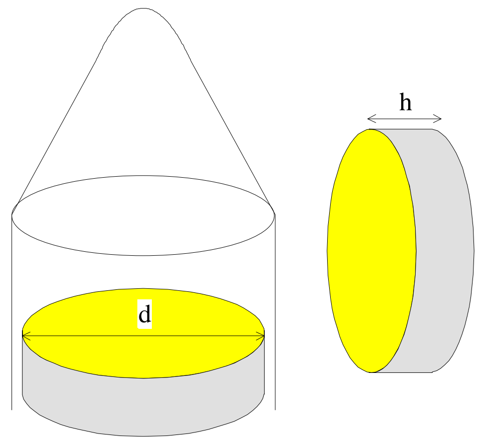

Launcher constraints. Vega: Top surface: 4.4 m²; Height: 0.46m; Volume: 2 m³. Rokot: Top surface: 3.5 m², height: 0.52m; Volume: 1.8 m³

Figure 3.4-5 : Accommodation of two cylinder-shaped satellites in the launcher fairing

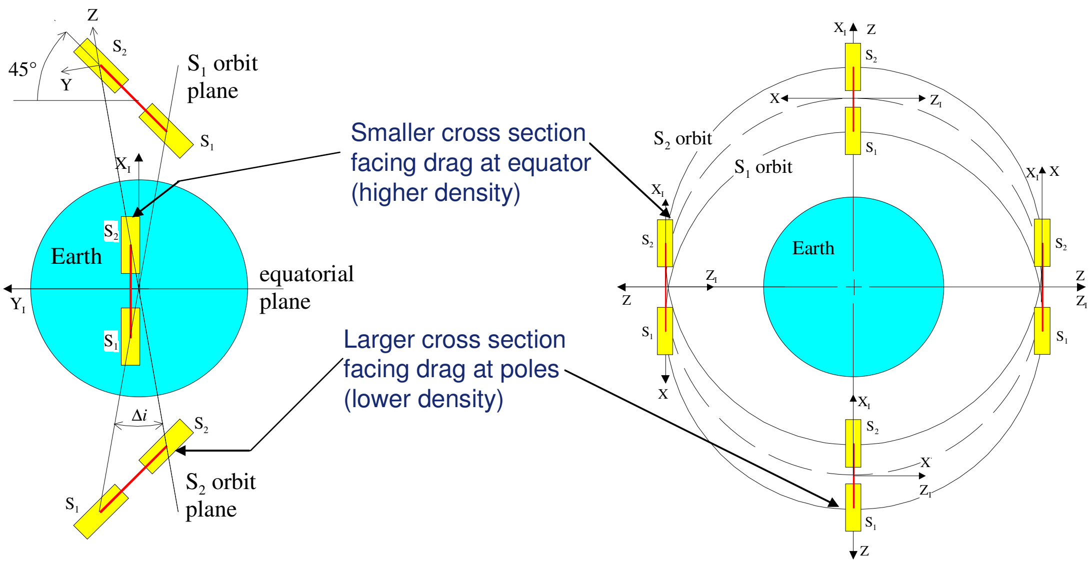

Prismatic shape for pendulum formation

Prismatic shape for N-S cartwheel formation

Figure 3.4-6 : In high-inclination orbits, the air density changes by factor of 3 from equator to poles. A prism-shaped satellite may minimize the variation of the drag force by matching the surface area ratio to the density ratio.

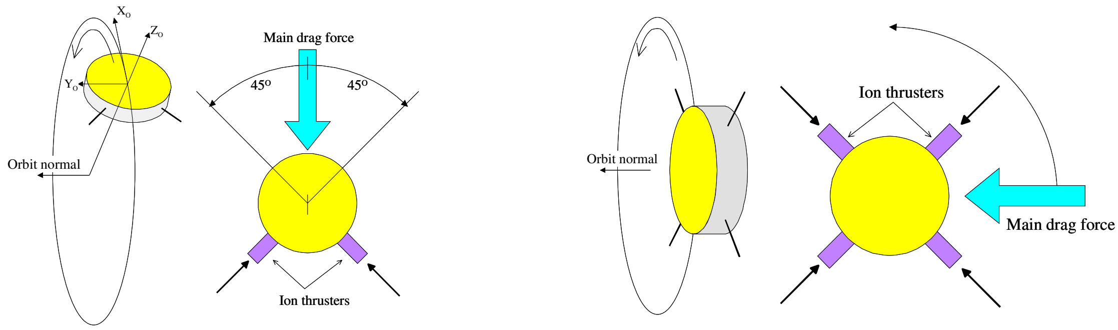

Pendulum **Cartwheel**

Figure 3.4-7 : In pendulum and cartwheel constellations, the drag force rotating around the body suggests the shape of a flat cylinder. The minimum number of thrusters for drag compensation is 2 (pendulum) and 4 (cartwheel).

3.4.4 Electrical Power

A comparison of GOCE and GRACE illustrates the impact of the orbit type and power demand on an NGGM.

GOCE is designed for sun-synchronous orbit (SSO) with maximum eclipse duration at the given altitude of 28 minutes (1 long eclipse season per year). The design includes the possibility, if needed, of a power limitation (hibernation) during the long eclipse season. The maximum power demand is driven by the ion propulsion which accounts for about 70% of the 1kW power budget at maximum thrust (20 mN). The range of variation of the sun incidence angle on the solar array is small (30°) and the array efficiency (all included) is about 150 W/m² (using GaAs solar cells). The power system density is about 7.5 W/kg and the power system mass fraction at launch about 13%.

The GRACE orbit is polar and the maximum eclipse per orbit is 36 minutes. Eclipses occur nearly all-year long with the exception of two short seasons (Figure 3.4-8). The power system operation bases on the array and battery working in tandem, the battery supplying the needed energy whenever the array power is insufficient (GOCE works on the same principle, but with much lower battery duty cycle). The power demand is very low, 160W, and the solar array efficiency (all included) is about 32 W/m² (Si cells). The power system density is about 1.5 W/kg and the power system mass fraction at launch is about 28%.

The power implications of a laser-based NGGM on a GRACE-like architecture are considerable. A large increase of the power demand must be expected (orbit maintenance by ion propulsion + laser system), as well as a mass increase (solar array & battery). Electrical power from fixed solar panels is likely to be insufficient for the laser system and the drag control (Figure 3.4-9), leading to either a steerable solar array (higher cost, disturbance to the measurements) or operational limits being introduced, with seasonal degradation of performance.

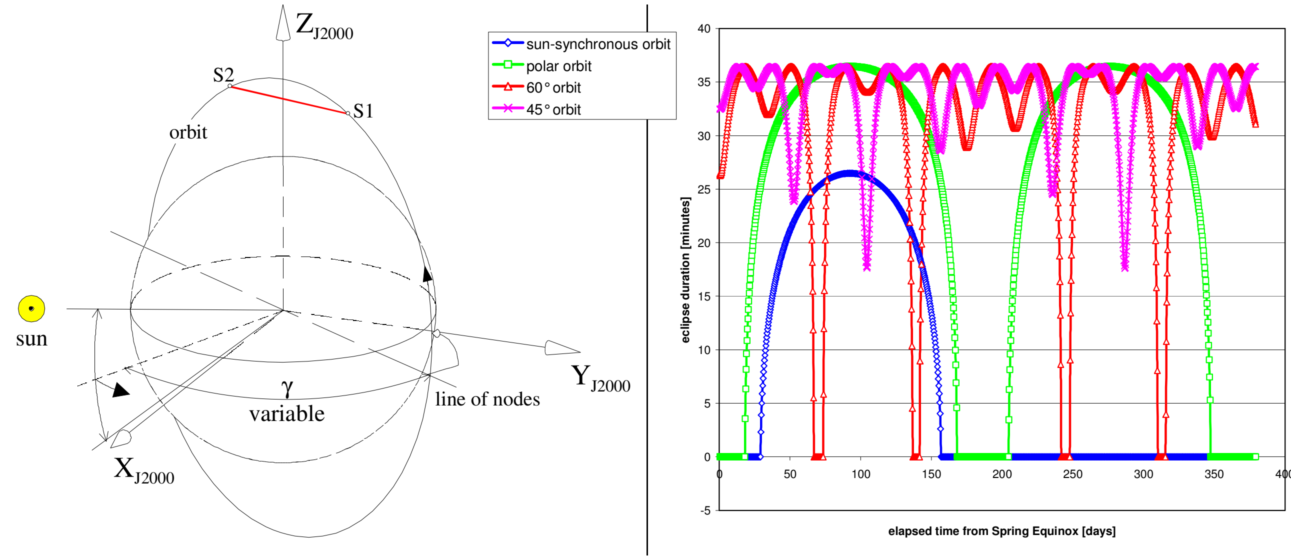

Figure 3.4-8 : In a non-sun-synchronous orbit, the sun revolves around orbit plane, leading to longer eclipses and longer eclipse seasons.

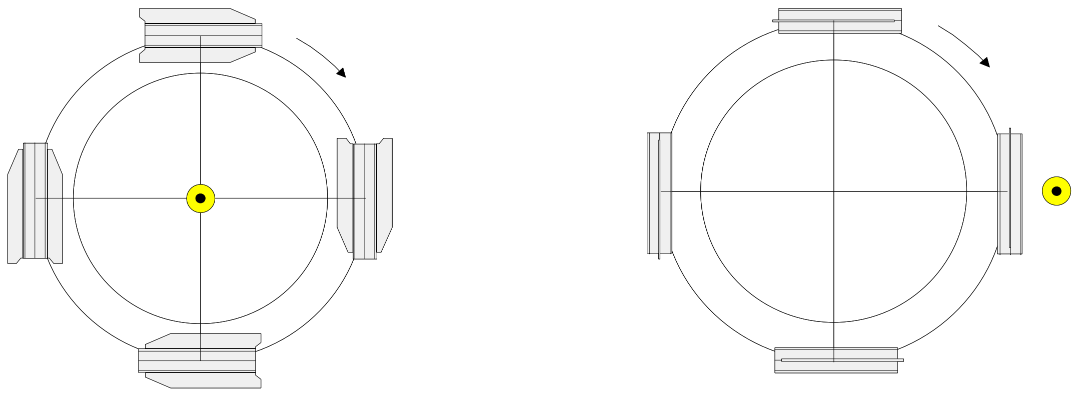

Season 1: sun normal to orbit, no eclipse

Season 2: sun in orbit plane, eclipse

Figure 3.4-9 : Example of GRACE-like formation with ~8 m² side panel (GOCE) + 1m² panel on top & bottom. The average active solar panel area decreases from 8 m² (1600 W) to 3 m² (590 W)

3.4.5 Telecommunications

In both GOCE and GRACE the TT&C is not particularly demanding. Both use S-band up- and down-links. GOCE uses one high-latitude ground station with a regular pattern of 1 pass each orbit. The telemetry generation rate is 14 kbit/s and the transmit rate on ground station passes is 1.2 Mbit/s. The antennas maintain a favourable orientation to the vector to the ground station, leading to small RF transmit power being used (250 mW).

GRACE uses two mid-latitude S-band stations, each satellite being operated individually, with different up/down frequencies. The station latitude leads to 4-5 passes per day with 6-7 min duration. The telemetry generation rate is 16 kbit/s and the telemetry dump rate is 1 Mbit/s. 2 W RF transmit power is used.

In a laser-based NGGM, increased telemetry rates are likely due to the laser link auxiliary and housekeeping data and the ion propulsion h/k data. There is a trade-off of independent satellite operation (at an operations cost impact) vs. constellation command and control via a master satellite and an inter-satellite data link (with an autonomy design impact). Note that the intersatellite link is needed anyway for laser operation. In the latter case, issues of frequency separation, polarization etc. must be addressed.

3.4.6 On Board Data Handling

The GOCE OBDH handles diverse functions (data handling proper, drag free and attitude control, active thermal control), leading to a system of moderate to high complexity. The performance (10 Hz DFAC control, 4Mbyte RAM load at 80%, CPU Load above 80%) is at the limit of the adopted standard (ERC32, 17 MIPS). The autonomy requirements are high (8 day autonomy, complex FDIR implemented in software and on board control procedures). The data Storage and routing requirements are moderate (< 20 kbits/s average data rate, 2x4 Gbit data storage). The radiation environment is not severe (<1 krad dose) whereas the EMC requirements are demanding in the L1-L2 bands. The interfaces are based on a Mil-1553 bus and an integrated RTU with a large number of I/O. The AOCS interface, in particular, includes the star trackers (serial), the mag torquer drivers, the RTU I/O for CESS-Sun Sensor, and the magnetometers.

The GRACE OBDH is not well known by TAS-I but the information available points to a not very complex system, based on a 1750 processor and with 1.4 Gbit data storage. An USO is employed with clock stability of 10 ms per 30 min.

In a laser-based NGGM, system capabilities close to GOCE will have to be implemented, due to the enhanced (w.r.t. GRACE) attitude control requirements. A processor upgrade w.r.t. GOCE will be necessary is DFAC is implemented. The autonomy requirements will be moderate to high (formation keeping and autonomous orbit maintenance; non-critical altitude control).

3.4.7 On Board Controls

In order to fully exploit the potentiality of a gravity mission based on the ll-SST technique and realized with a laser interferometer and ultra sensitive accelerometers, several controllers must be put in place:

- linear drag-free;
- orbit;
- formation;
- attitude and angular drag-free;
- laser beam pointing.

The implementation of all these controllers, which must work in a synergetic way, contributes to the overall system complexity (and costs). The possibility of simplifying the system by dropping some of these controllers (drag-free, laser beam pointing) is one of the tasks to be addressed during the study.

Drag Free Control

Linear drag-free control has the task of reducing the dynamic range of the measured acceleration. This is necessary for both instrument feasibility (sensor and electronics accuracy versus range) and to reduce the impacts of accelerometer nonlinearities and misalignments on overall instrument accuracy after in-flight calibration.

According to current mission architecture, the residual linear acceleration shall be < 10^{-6} m/s² (max. value) and 10^{-8} m/s²/$Hz^{-1/2}$ in the [0.001, 0.01] Hz band, that is, each axis shall be controlled.

Drag-free control requires throttlable thrusters with dynamic range compatible with the different environmental conditions (operating altitude, solar activity). This is very expensive in terms of fuel mass. Since the scientific requirements, and consequently the requirements of the fundamental observables, will be reviewed during the study, even the conclusions on the drag-free control might change.

Orbit Control

Orbit control shall keep the average formation altitude and perform, if required, correction of secular trends affecting the inclination, node or argument of pericentre. The rationale and requirements are discussed in §3.4.2. Autonomous altitude control will be traded vs. ground-based control.

Formation Control

Formation control shall provide the capabilities for both formation acquisition and maintenance, and an anti-collision strategy. Formation keeping control shall maintain the formation geometry during the observation phase in a box with sizes (assuming 10km average satellite distance) < 500m along track, < 50m across track, < 50m radial.

The challenge of the formation control for this mission consists in keeping the relative motion within these boundaries without interfering with the scientific measurements, operating in synergy with the drag-free control and minimizing the thrusters use (in terms of dynamic range, propellant consumption).

Attitude Control

According to the current architecture, attitude control shall:

- maintain the attitude errors with respect to the LORF compatible with laser beam pointing range;
- constrain the angular accelerations and the angular rates to be very stable (<10^{-8} rad/s² $Hz^{-1/2}$ and < 10^{-6} rad/s $Hz^{-1/2}$ respectively in the [0.001,0.01] Hz band.

The latter requirement arises because the coupling of angular accelerations and angular rates with the accelerometer displacement from the satellite COM produces a linear acceleration which contributes to the measurement error of the non-gravitational accelerations of the satellite COM. The above requirements have an impact on the closed loop attitude control and on the reference attitude trajectory to be tracked.

Laser Beam Pointing Control

Laser beam pointing control is used to guarantee the optical link between the satellites (acquisition and tracking). The orientation of the laser beam towards the retro-reflector on the other satellite must be very precise and stable (< 10^{-5} rad and < 10^{-7} rad $Hz^{-1/2}$ respectively).

The presence of a continuously operating Beam Steering Mechanism (BSM) on a long-duration mission is certainly a weak point, besides being a potential source of disturbance for the accelerometer measurements. The BSM can be removed if all its tasks can be handed over to the satellite attitude control. These tasks can be facilitated if the pointing requirements can be relaxed and if the laser beam divergence can be increased. On the other hand, tracking this oscillation by changing the attitude of the satellite could conflict with the attitude stability requirements on angles, angular rates and angular accelerations. These issues will be addressed during the study.

3.4.8 Formation Keeping

The formation control requirements are not very stringent (loose formation flying). The "control box" inside which the motion of Satellite 2 relative to Satellite 1 must be bounded is established by the working range for which the optical metrology system has been sized. The sides of the control box have been established as follows (d = 10 km): 500 m w.r.t. the nominal distance along the line joining the two satellites; 50 m in the transversal directions (Figure 3.4-10). In case of a cross-line formation (cartwheel, pendulum) the control box applies to each point of the nominal relative trajectory and defines the maximum acceptable deviation from it.

The challenge of the formation control consists in keeping the relative motion within these boundaries without interfering with the scientific measurements, operating in synergy with the drag-free control and minimizing the thrusters use (in terms of dynamic range, propellant consumption).

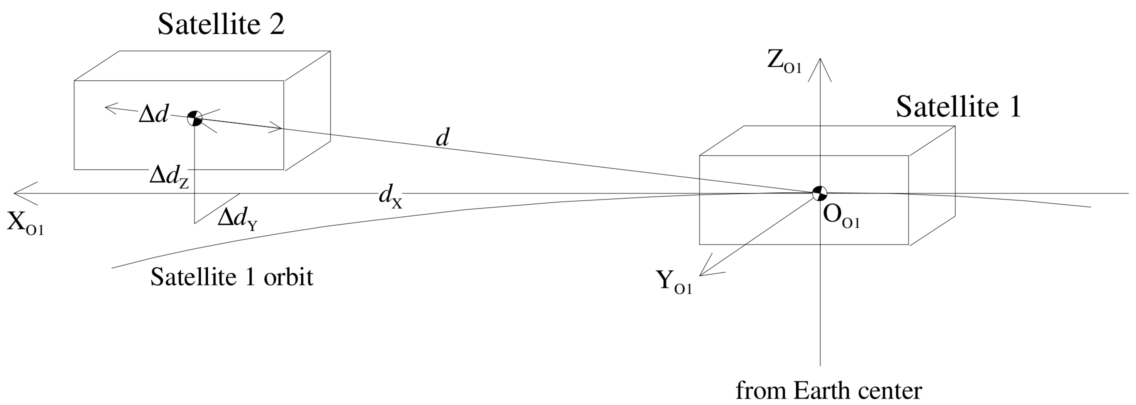

Figure 3.4-10 : Definition of the control box of Satellite 2 in the Satellite 1 LORF

The formation controller is designed according to the following criteria:

- The forces applied to the satellites for maintaining their relative motion bounded change their relative distance. Since the distance variation between satellites is a fundamental observable for the reconstruction of the gravity field, the formation control action must operate below the science bandwidth of 1 mHz (i.e. the satellites must be “free” to move under the effect of the gravity field over time scales of 1000 s).
- The formation control accelerations must fulfil the drag-free requirements, if any (in any case, the formation control action shall not cause saturation of the accelerometers).
- Differential bias and drift between the accelerometers in the two satellites shall be estimated and removed from the thruster commands.
- The effect of differential eccentricity of the orbits and of the main gravitational harmonics (in particular J2) which perturb the inter-satellite distance but do not cause violation of the formation control requirements shall not be compensated.

Different formation geometries give rise to different formation control requirements. The time evolution of the inter-satellite relative state is an indicator of the long-term formation stability.

Both the in-line, in-plane formation and the cartwheel formation are basically stable under the effects of gravitational perturbations alone (Figure 3.4-11 and Figure 3.4-12). A pendulum formation, instead, is subjected to a small secular orbit plane drift (Figure 3.4-13) which must be compensated. Further (small) orbit adjustment requirements will arise from non-gravitational perturbations.

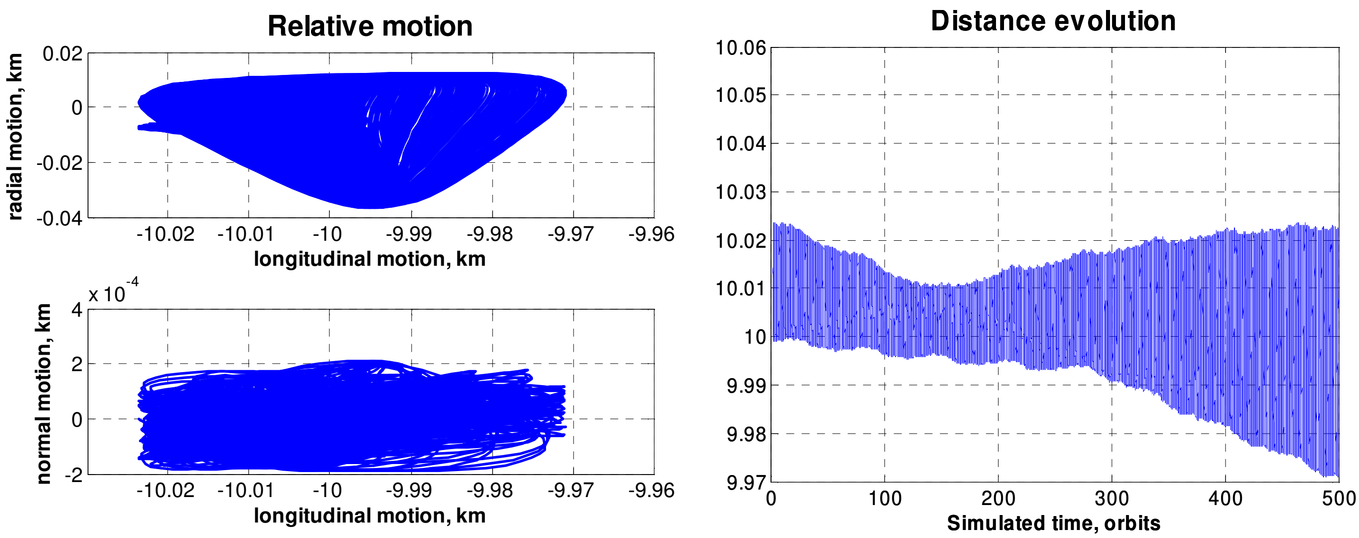

Figure 3.4-11: Mid-term evolution (1-month) of an in-line formation

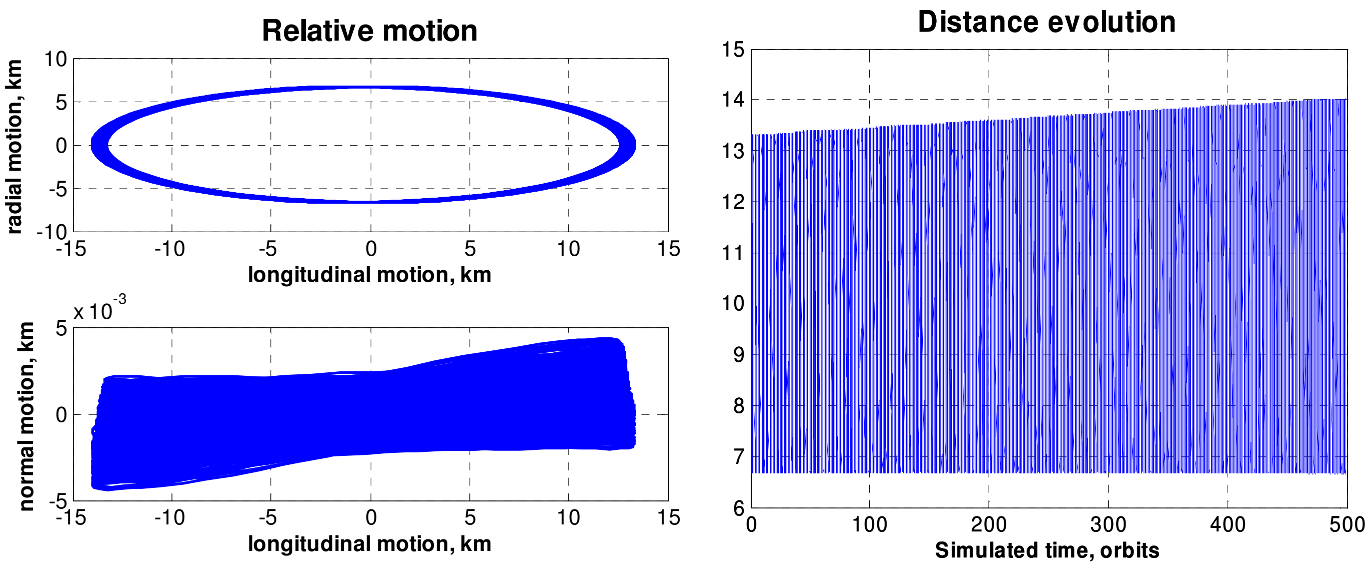

Figure 3.4-12: Mid-term evolution (1-month) of a Cartwheel formation [325km mean altitude, a = 6703 km, e = 4.973e-4, 180º argument-of-perigee shift]

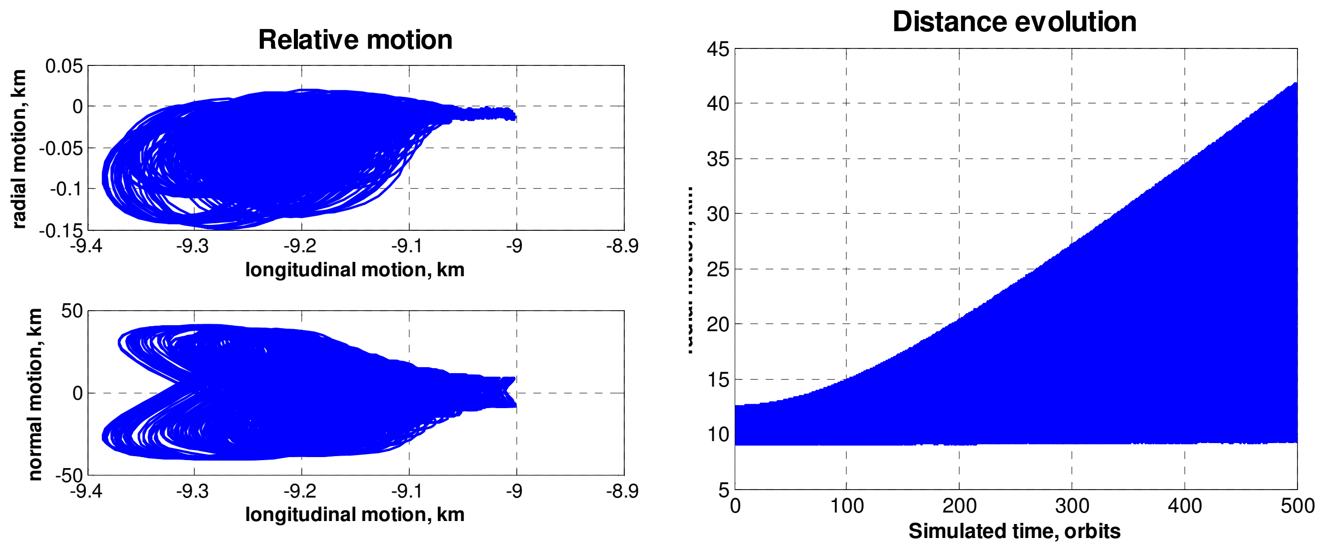

Figure 3.4-13: Mid-term evolution (1-month) of a Pendulum formation [initial conditions: Δi = 0.074º, ΔM = ~0.08º]

3.4.9 Summary

This review points to a considerable increase of complexity on the way from the existing GRACE to a laser-based NGGM:

- Increased launch mass, power demand and telemetry rate
- Addition of an intersatellite data link
- GaAs-cell based solar array

- On board processor upgrade
- Ion propulsion for orbit maintenance
- Drag-free control (TBC)
- Precise pointing control (either by BSM or by satellite)
- Enhanced formation control (laser requirements and compensation of instable formation geometries).

4. PROPOSED TRADE-OFF APPROACH

4.1 Parameters identifying a mission architecture and proposed range of variation

The parameters identifying a mission architecture include:

- Number of orbits
- Orbit elements (altitude, inclination, period, repeat cycle)
- Number of satellites per orbit
- Mission duration
- Type of satellite formation (in-line, pendulum, cartwheel, gravity wheel, other)
- Intersatellite distance
- Gravity field measurement technique (SST alone, SST + gradiometry)
- SST metrology performance
- Accelerometer performance for non-gravitational accelerations.

Table 4.1-1 and Figure 4.1-1, Figure 4.1-2 show the proposed range of variation of these parameters to be addressed in the forthcoming studies.

Table 4.1-1 : Range of variation of mission parameters

Item	Lower limit	Upper limit	Rationale
Altitude	300 km	400 km	Limited from below by cost of orbit maintenance, limited from above by measurement resolution.
Inclination	60°	97°	Lower limit by latitude coverage, upper limit = SSO
Lifetime		6 yr	Half a solar cycle
Inter-satellite distance	1 km	100 km	@ 1 km, overall performance limited by non-gravitational acceleration measurement noise; @ 100 km, overall performance limited by distance measurement noise
SST metrology performance $\delta L/L$	5.0E-13 $m/m/Hz^{1/2}$	5.0E-12 $m/m/Hz^{1/2}$	Flat part of the spectrum, see Figure 4.1-1. The lower limit corresponds to the previous NGGM study, the upper limit to 10 times the previous limit. With the top-level requirement relaxed by a factor of 10, there is a potential significant simplification of the payload and system design (e.g. no laser beam pointing device, no lateral drag-free control).
Acceleration measurement performance	0.1E-10 $m/s^2/Hz^{1/2}$	1.0E-10 $m/s^2/Hz^{1/2}$	Flat part of the spectrum, see Figure 4.1-2. The lower limit corresponds to the previous NGGM study, the upper limit to 10 times the previous limit.

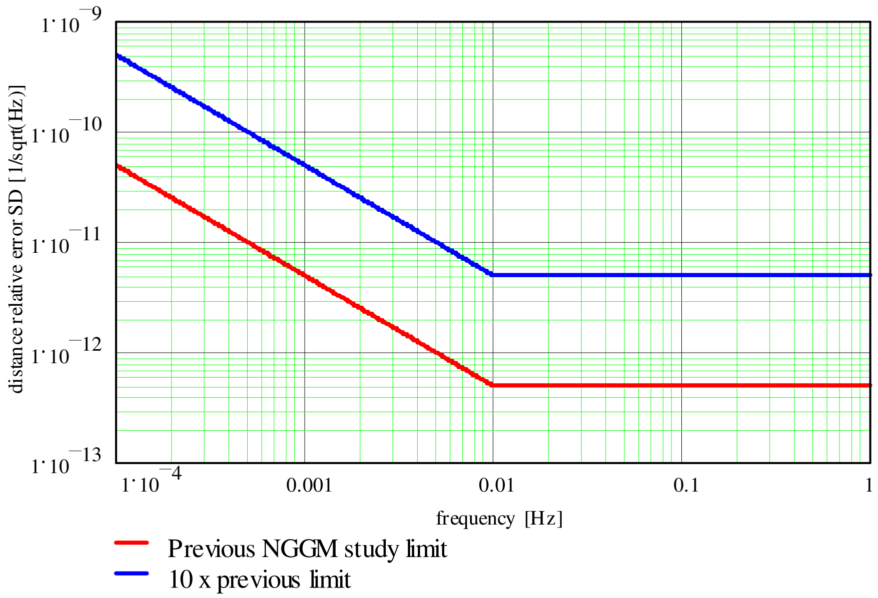

Figure 4.1-1 : Proposed range of variation of the relative distance error

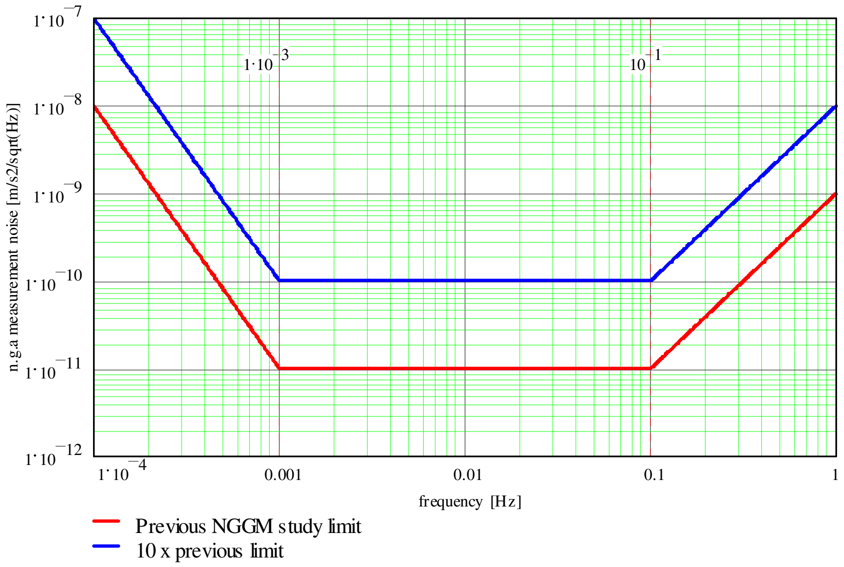

Figure 4.1-2 : Proposed range of variation of the acceleration measurement error

4.2 Candidate mission architectures

The architectures to be addressed include the 2-satellite formations mentioned many times in this report (in-line, cartwheel, pendulum), plus possibly formations with n>2 satellites (n-wheel). One and two pairs (or multiplets if n>2) will be addressed. The orbit candidates are generically identified by SSO, polar and mid-latitude (elements to be specified on a case by case basis).

The combinations of these parameters are depicted in Table 4.2-1. The combinations highlighted in light blue indicate some sort of priority, according to the following approach:

1. The first objective will be to establish the potential assets w.r.t. GRACE, and the ultimate limits, of an architecture comprising one satellite pair only. This architecture remains the most likely, if only for reasons of cost. The analysis will proceed from the simplest configuration up (in-line SSO, then in-line non-SSO, then cartwheel, pendulum, …). The performance index will be the ability to (partially) remove the GRACE drawbacks by (a) increased SST resolution, (b) better orbit control, (c) better attitude control, (d) different orbit, (e) gravity sampling in different directions, …
2. After the first step is done, 2-sat-pair architectures will be analyzed, again, from the simplest configuration up (2 pairs in the same orbit, shifted in mean anomaly; 2 pairs in different orbits, shifted in inclination; etc.)
3. The process will stop when either the performance is satisfactory or a “cost” upper limit is reached.

Table 4.2-1 : Mission architecture combinations

Sat pairs	1	2		
Orbit	SSO	Polar	Mid-inc	
Formation type	In line pair	pendulum	cartwheel	n-wheel

Combinations	1	In line pair		SSO Polar Mid-inc			*GRACE+*
		pendulum cartwheel n-wheel	X	SSO Polar Mid-inclination			
	2	In line pairs		SSO Polar mid-inc	+ + +	SSO Polar mid-inc	M-shift
				SSO	+	Polar	
				SSO	+	mid-inc	
				Polar	+	mid-inc	*Bender*
		cross-line pairs	X	different orbits			

4.3 Mission architecture ranking

The objective of the study is to select a mission architecture that achieves the best (according to criteria to be defined) balance of performance and cost. Performance will be defined by the scientific institutes participating in the study, with respect to the known performance of GRACE, in terms of indices such as latitude coverage, reduction of aliasing, reduction or elimination of systematic distortions, etc. “Cost” may be defined in several ways which, eventually, all boil down to cost without inverted commas. In order to make the “cost” assessment as objective as possible, use of a cost model is proposed as detailed in §4.4.

The assessment of performance and cost will end up in a ranking such as the one depicted (for now, in a qualitative way) in Figure 4.3-1.

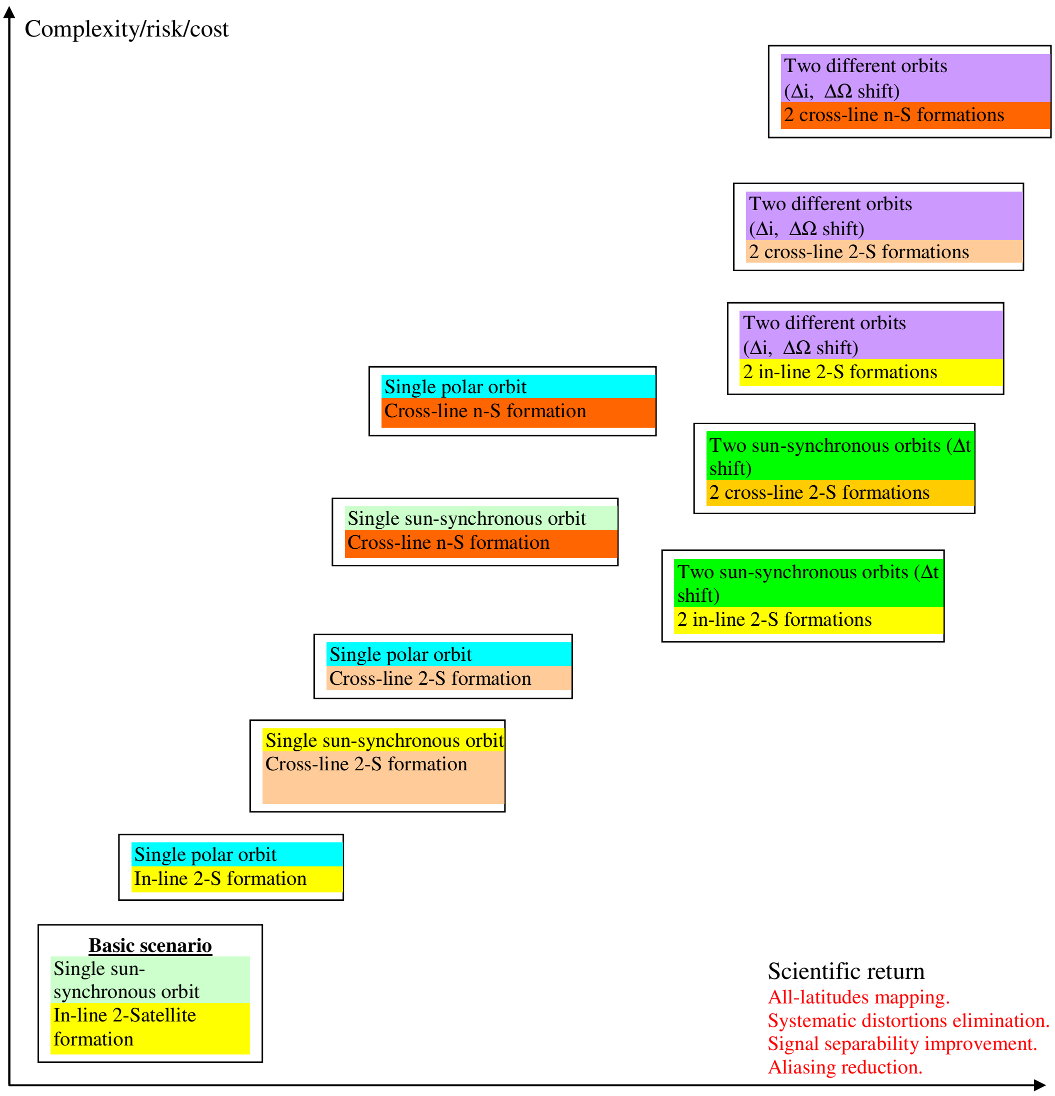

Figure 4.3-1 : Qualitative ranking of mission options in terms of increasing level of complexity/ risk/ cost and scientific return (n-s = n-Satellite, n>2).

4.4 Satellite cost model

A simple linear spacecraft cost model was published by L. Sarsfield of the Critical Technologies Institute, Rand Corporation, in 1998[1]. The main attraction of the model is that it was calibrated on a sample of 14 NASA missions of the 1990's, the cost of which was made available to the author of the model. Complete data for a similarly large sample of European missions is not readily available, therefore the US model "as is" was tried for suitability to our purposes.

In this model, the spacecraft cost is estimated as function of s/c dry mass times a "Factor of Complexity" (Fc). Note that the procurement cost only is used, excluding launch, ground segment etc.. Fc is the unweighed average of 11 deterministic indices, each of them projected on a scale of 1 to 5:

- On-Orbit Design life [yr]
- Destination orbit [No. of implied failure modes]
- S/c dry density [kg/m³]
- Payload dry mass fraction [%]
- Bus Pointing Accuracy [deg]
- Solar array efficiency BOL [W/m²]
- Power system density [W/kg]
- Telemetry data rate [kbit/s]
- On board Processing power [MIPS]
- Mass memory size [Mbit]
- Lines of SW code [k lines].

The scaling is made by finding the minimum and maximum in the sample of each index, and projecting the number proportionally on a scale of 1 to 5. Note that all of these indices are hard numbers: no qualitative judgements are implied, making the index as "value-free" as desired.

Further necessary qualifications are as follows:

- The model is geared to a sample of small/medium missions of the 90's. The indications are that it would fail to give consistent cost predictions if used for larger missions
- Some of the indices are outdated, e.g., the upper limit of the mass memory in the sample is 2 Gbit, which might have been state of the art for small sats in the mid nineties but is certainly no limit today
- For comparisons with European satellites, we use the assumption that 1 US$ = 1 €, and we do not correct for inflation. The former assumption is common when purchasing power is concerned. The latter is considered included in the model error (≈30%).

The compilation of indices for GOCE and GRACE is in Table 4.4-1. The model appears to fit quite well GOCE and GRACE (Figure 4.4-1). This is not unexpected of GRACE, which belongs to the same environment and epoch as the original sample. GOCE is at the upper limit of the range but anyway within 10% of the linear fit [note that if the model were corrected for inflation, GOCE would be well below the linear fit, i.e., a bargain for ESA…]. We conclude that the model is adequate for our purposes, especially since it will be used for comparisons, rather than for absolute cost estimations.

[1] www.rand.org/pubs/monograph_reports/2009/MR864.pdf

Table 4.4-1 : Complexity indices of GOCE and GRACE

System Driver	Reference [GOCE] Value	CF 1 to 5	Reference (GRACE) Value	CF 1 to 5
On-Orbit Design life [yr]	2.4	2.0	5	3.9
Orbit altitude [km]	260 DFC	3.7	450	2.1
Payload dry mass fraction [%]	19.3%	1.9	5.4%	1.0
S/c dry density [kg/m³]	172.7	3.1	188.8	3.3
Bus Pointing Accuracy [deg]	3	1.0	0.05	4.2
Solar array efficiency BOL [W/m²]	148.2	2.7	32	1.0
Power system density [W/kg]	7.4	1.4	1.5	1.0
Telemetry data rate [kbit/s]	1200	2.6	1000	2.3
On board Processing power [MIPS]	17	4.2	5	1.8
Mass memory size [Mbit]	8000	5.0	1400	3.8
Lines of SW code [k lines]	320	4.5	30	1.8
Average complexity		**2.9**		**2.4**

GRACE data based on Dec. 1997 proposal estimated

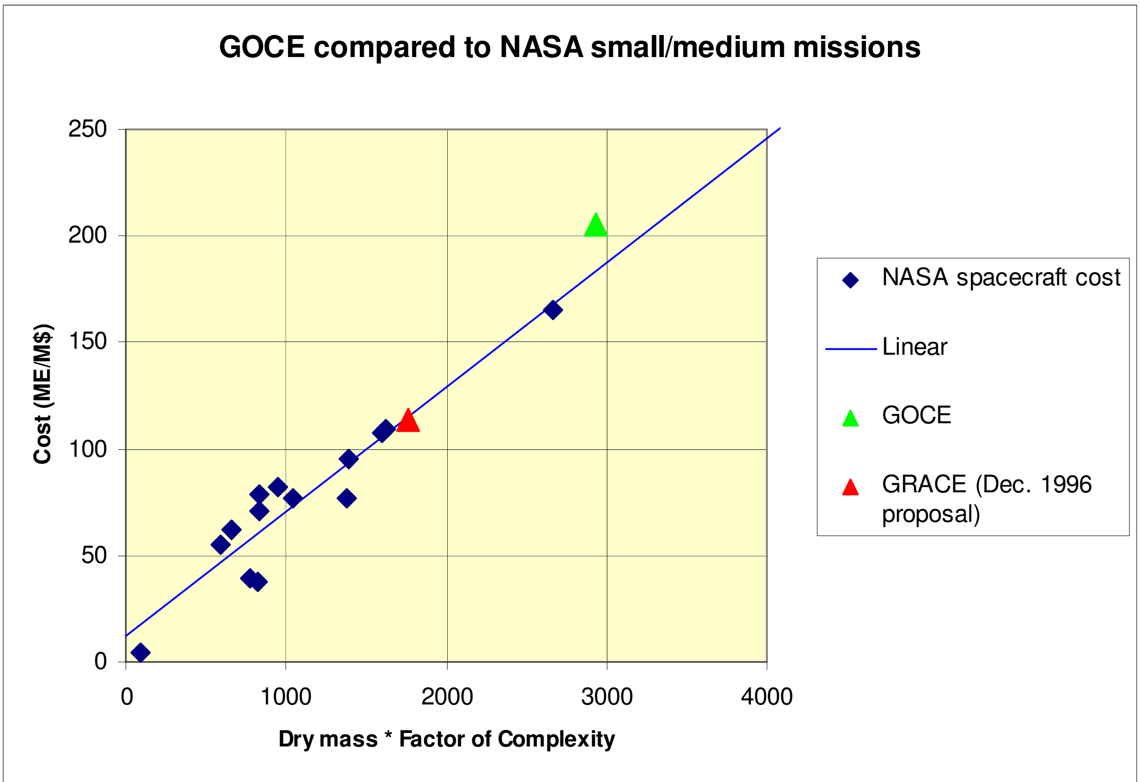

Figure 4.4-1 : Application of cost model to GOCE and GRACE

5. ACRONYMS

AD	Applicable Document
BOL	Beginning of Life
BSM	Beam Steering Mechanism
C/C	Carbon-Carbon (composite)
CHAMP	CHAllenging Minisatellite Payload
COM	Centre of Mass
E2ES	End-to-End Simulator
EOL	End of Life
FF	Formation Flying
GNSS	Global Navigation Satellite System
GOCE	Gravity field and steady-state Ocean Circulation Explorer
GPS	Global Positioning System
GRACE	Gravity Recovery And Climate Experiment
INRIM	Istituto Nazionale di Ricerca Metrologica
ITT	Invitation To Tender
KBR	K-Band Ranging
LEO	Low Earth Orbit
ll-SST	low-low Satellite to Satellite Tracking
LORF	Local Orbital Reference Frame
LRR	Laser Retro Reflector
MBW	Measurement Bandwidth
MST	Mission Simulation Tool
NGGM	Next-Generation Gravity Mission
P/L	Payload
POD	Precise Orbit Determination
PSD	Power Spectral Density
RD	Reference Document
RF	Radio Frequency
RMS	Root Mean Square
S/C	Spacecraft
SLR	Satellite Laser Ranging
SQUID	Superconducting Quantum Interference Device
SSO	Sun Synchronous Orbit
SST	Satellite to Satellite Tracking
TAS-I	Thales Alenia Space Italia
TBC	To Be Confirmed
TBD	To Be Defined

END OF DOCUMENT